ORIGINAL ARTICLE

# Effect of Lubricant on Wear Behavior of Ultrahigh-molecular-weight Polyethylene Cups Against Zirconia Head in Hip Joint Simulator

**Masami HASHIMOTO[1], Mineo MIZUNO[1], Satoshi KITAOKA[1], Hiroaki TAKADAMA[2], and Masaru UENO[3]**

[1] *Japan Fine Ceramics Center, Nagoya, Japan*
[2] *Chubu University, Nagoya, Japan*
[3] *Japan Medical Materials Corporation, Osaka, Japan*

**Synopsis**

The wear behavior of a femoral head made of zirconia ($ZrO_2$) against an acetabular cup made of ultrahigh-molecular-weight polyethylene (UHMWPE) was investigated using a hip joint simulator for five types of lubricants. Five types of lubricants were used: balanced salt solution (BSS), a BSS solution containing bovine serum albumin (A) and γ-globulin (G) (BSS+A+G), and a BSS solution containing 1.5 times the concentrations of A and G (BSS+1.5(A+G)), as well as two types of bovine sera (CS1 and CS2). The effect of the total protein concentration in the lubricant on the wear rate was assessed. The weight loss of the UHMWPE cup was measured. Weight loss increased with the test duration for all lubricants except for BSS. The lubricant that produced the highest wear rate (mg/$10^6$ cycles) calculated from the weight loss during the test, was BSS+1.5(A+G), followed by BSS+A+G. Little weight change of the UHMWPE cup was observed for BSS. The wear rate increased with the concentration of protein, irrespective of the protein species. During the experimental observation period, the wear rate decreased in the order CS1 > BSS+1.5(A+G) > CS2 > BSS+A+G > BSS $\simeq$ 0. The comparison of quantitative measurements of individual particles in the lubricants showed that the morphology of each type of particle was dependent on the type of lubricant. Fibers and/or granules appeared in CS1 and CS2. In contrast, elongated fibers were mainly generated in BSS+A+G and BSS+1.5(A+G). These elongated particles formed by wear suggest that an adhesive mechanism, rather than the abrasive mechanism associated with asperities, was active. Our results suggest that the adhesive mechanism was active in lubricants containing proteins such as A and G.

***Key words:*** *hip joint, wear, hip simulator, lubricant, polyethylene debris*

## Introduction

The ultimate goal in the design of a hip joint wear simulator and the associated test protocol is to reproduce the type and amount of wear that occur clinically. Commonly used hip simulators vary markedly in load and motion characteristics [1–3], and use various lubricants, including distilled water, physiological saline, blood serum, synovial fluid, mineral oil and synthetic serum. Comparative studies have shown that the type and amount of wear that occur in physiological lubricants (i.e., serum and synovial fluid) more

closely resemble those occurring *in vivo*, probably partly due to boundary lubrication by proteins [4–7]. It has also been shown that the type and amount of wear vary with the type of protein present in the lubricant and the concentration of the protein [8, 9].

At present, the international standard recommends calf or bovine serum that is pure or diluted with distilled water as the best substitute for synovial fluid in *in vitro* tests, but there is not complete agreement concerning this choice. In fact, the protein concentration of various commercially available serum products varies over a wide range (40-80 mg/ml) and the protein concentration of lubricants has a marked effect on the friction and wear of tribological pairs used in prosthetic joints. It is not easy to achieve reproducible results or to compare the results obtained by different laboratories. Therefore, it is desirable to develop, as an alternative to bovine serum, a stable and reliable lubricant whose composition can always be set to a specified value at the beginning of a wear test.

We previously prepared several lubricant solutions composed one or more of the major components in bovine serum, such as bovine serum albumin (A), γ-globulin (G) and a lipid with some additives [10]. The change in weight of the ultrahigh-molecular-weight polyethylene (UHMWPE) cups was dependent on the component. In the case of a one-component lubricant solution, the weight change revealed that the G solution produced the largest wear rate, but lecithin solution produced a lower wear rate than bovine serum. The weight change in two-component solutions containing A and G was similar to that in bovine serum. Moreover, the two-component solution containing A and G was stable. Therefore, this solution may serve as a particularly good model solution for the study of the wear properties of the hip joint. Owing to the importance of the particle characteristics in the quantity and quality of biological responses, great emphasis has been placed on developing techniques for extracting and studying the quantity, size and morphology of UHMWPE wear particles [11, 12].

In this study, we investigated the wear behavior of a zirconia ($ZrO_2$)/UHMWPE coupling in a two-component solution containing A and G using a hip joint simulator. The effect of the type of lubricant on the wear properties and the morphology of the wear debris was also investigated.

## Materials and Methods

### *1. Materials and hip simulator*

The wear behavior of a $ZrO_2$/UHMWPE coupling was investigated using a hip joint simulator. A $ZrO_2$ femoral head component with a diameter of 26 mm (Japan Medical Materials Corp., Osaka, Japan) was used. The $ZrO_2$ was 3 mol% yttria - doped tetragonal zirconia polycrystalline (3Y-TZP). The UHMWPE acetabular cup used was a commercially available component used in surgical implants (Japan Medical Materials Corp.). The inner and outer diameters of the UHMWPE cup were 26 and 50 mm, respectively. Two couplings were prepared for each condition.

A 12-station hip joint simulator (MTS Systems Corp., MN, USA) was used in the wear test. In the simulator, the acetabular cup was mounted above the femoral head in an upright position (Fig. 1). Motion was imparted to the femoral head through an inclined rotating bearing block. This produced a cross-path pattern at all fixed points on the articular interface. A physiological

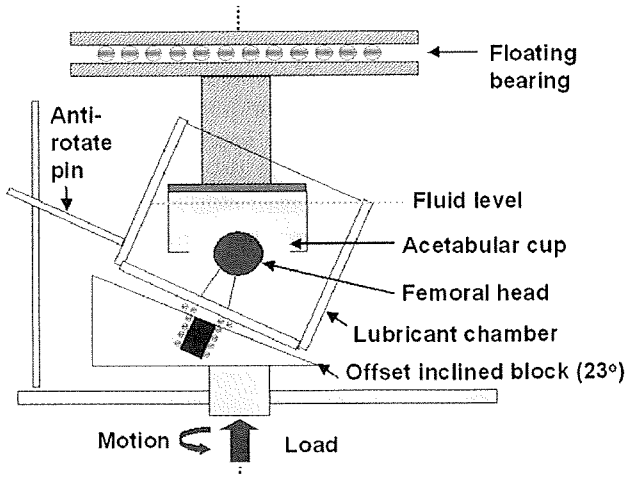


**Figure 1** Schematic diagram of the MTS hip joint simulator.

cyclic load was applied to the acetabular cup via a hydraulic acutuator mounted below the inclined block. Loads simulating a physiological loading curve with double peaks of 1.8 and 2.8 kN were applied. Loading and motion were synchronized at 1 Hz. Both the head and cup were completely immersed in 750 ml of fluid. The compositions of the prepared artificial lubricants are listed in Table 1. They were prepared by dissolving reagent-grade A and G (Nacalai Tesque, Inc., Kyoto, Japan) into a phosphate buffered saline with tri-sodium hydrogen ethylene diaminetetraacetate (3Na-EDTA) (Nacalai Tesque, Inc.) and sodium azide ($NaN_3$) (Wako Ltd., Osaka, Japan). 3Na-EDTA and $NaN_3$ were added to stabilize the proteins in the solution and to keep the pH close to that in the body. The concentrations of NaCl, $Na_2HPO_4$, 3Na-EDTA and $NaN_3$ were set at 0.8%, 10 mM, 20 mM and 0.1%, respectively. The concentration of each protein in the solutions except BSS+1.5(A+G) was set at 25% of that of human serum in accordance with ISO 14242-1, while the concentration of BSS+1.5(A+G) was set at 1.5 times of that of BSS+A+G solution. As a reference, the base lubricants used were phosphate buffered saline and calf sera from two companies: Sigma-Aldrich Japan (Tokyo, Japan) (CS1) and BioWest (Nuaill, France) (CS2) (Table 1). A mixture of 25 vol% bovine serum, 20 mmol/L of ethylene diamine tetraacetic acid (EDTA), and 0.1 mass% sodium azide was used as a lubricant, in accordance with the ISO-14242-1 standard. Testing was performed until 5.0 x $10^6$ cycles were completed.

### *2. Wear characterization*

All the lubricants were changed after every 0.5 x $10^6$ cycles during the tests. When the lubricant was changed, all the cups were cleaned, dried and weighed using an electronic balance (resolution: 0.01 mg) to determine the weight loss. The cups were washed using a four-step procedure. First, the cups were cleaned in an ultrasonic bath for 10 min with a soap-water solution. Second, the cups were ultrasonically cleaned in deionized water for 10 min. Third, the cups were ultrasonically cleaned in ethanol for 10 min. Lastly, the cups were vacuum-dried for 30 min to remove excess water from the surface. The net weight losses for each cup were plotted against the number of test cycles.

### *3. Debris extraction and SEM*

A sample of each lubricant used in the test was obtained when the simulators were stopped for the gravimetric analysis of wear performance. From the 750 ml lubricant bath, 10 ml was taken during digestion and debris extraction. The homogeneity of the lubricant was ensured by agitating it prior to sampling. In each case, synovial fluid was digested using the same amount of 10 M sodium hydroxide at 65 °C for 3 h, added to a sucrose (1.2 g/ml) and isopropyl alcohol (0.919 g/ml) solution with a density gradient in a 30 ml tube, and ultracentrifuged at 114,500 g at 4 °C for 3 h (Hitachi Koki Co, Ltd., Tokyo, Japan). The interface layer was collected and mixed with methyl alcohol in another 30 ml tube, and ultracentrifuged again at 114,500 g for 3 h. The bottom layer was added to sucrose (1.05 g/ml)

**Table 1** Concentrations of solutions in lubricants used in wear tests.

| Lubricant (mg/ml) | NaCl | $Na_2HPO_4 \cdot 12H_2O$ | Protein (Total) | Albumin | Globulin | | |
|---|---|---|---|---|---|---|---|
| | | | | | α-G | β-G | γ-G |
| BSS | 8 | 3.58 | 0 | 0 | 0 | 0 | 0 |
| BSS+A+G | 8 | 3.58 | 10.7 | 7.3 | 0 | 0 | 3.4 |
| BSS+1.5(A+G) | 8 | 3.58 | 16.2 | 11.1 | 0 | 0 | 5.1 |
| CS1 | *1 | 0 | 18.3 | 8.4 | 2.7 | 3.4 | 3.8 |
| CS2 | *2 | 0 | 15.5 | 7.8 | 2.3 | 4.0 | 1.4 |

*1 Na 3.38 mg/ml, *2 Na 3.24 mg/ml

and isopropyl alcohol solution (0.973 and 0.919 g/ml) with a density gradient and ultra-centrifuged again at 114,500 g for 3 h. UHMWPE debris was collected from the interface between the two layers and filtered through a 0.1 μm filter. The UHMWPE debris was examined using a JSM-633OF FE-SEM system (JEOL DATUM Co., Ltd., Nagoya, Japan) after coating it with a thin Au film.

### *4. Debris analysis*

Digital images of individual UHMWPE debris particles were extracted from archival scanning electron micrographs. UHMWPE debris analysis was conducted by computer using a customized application based on public-domain image-processing (3D Volume, RATOC System, Tokyo, Japan) and analysis programs (Image J, National Institute of Health, Maryland, U.S.A.). UHMWPE debris particles were outlined by binary image processing and analyzed to obtain six shape and size parameters for each particle: number, area (S), particle size (PS), equivalent circle diameter (ECD), aspect ratio (AR) and circularity (R). PS is the major diameter of the particle. ECD is a measure of the size, defined as the diameter of the circle with an area equivalent to the area of the particle, and has a unit of length. Thus, the area (S) of the particle is first determined using image analysis then ECD is calculated using

$$ECD=2(S/\pi)^{1/2}. \quad (1)$$

AR is the ratio of the minor diameter to the major diameter. R is a measure of how closely the particle resembles a circle, with a perfect circle having a value of 1. The distributions of the four shape and size parameters (PS, ECD, AR and R) were plotted. The mean values of these four shape and size parameters were also derived.

### Results

Figure 2 shows a plot of the cumulative weight loss of the UHMWPE cups as a function of test duration for the five lubricants. With the exception BSS, the weight loss of the cups increased with test duration. The total amounts of weight loss for BSS+A+G and BSS+1.5(A+G) after 5.0 x $10^6$ cycles were 61.3 and 87.2 mg, respectively. In the cases of the sera, the total weight loss for CS1 after 5.0 x $10^6$ cycles was 210.3 mg. In contrast, UHMWPE subjected to CS2 had a lower average wear rate throughout the test. After 5.0 x $10^6$ cycles in CS2, the total weight loss of UHMWPE was 64.6 mg. We defined the initial wear rate as that from the first cycle up to the 1.0 x $10^6$ th cycle and the steady wear rate as that from the 4.0 x $10^6$ th cycle to the 5.0 x $10^6$ th cycle. The following initial and steady wear rates were obtained: 13.1 and 15.7 mg / $10^6$ cycles for BSS+A+G, 15.1 and 20.7 mg / $10^6$ cycles for BSS+1.5(A+G), 27.9 and 47.3 mg / $10^6$ cycles for CS1, and 16.9 and 13.7 mg / $10^6$ cycles for CS2, respectively. These results revealed that BSS+1.5(A+G) exhibits relatively similar wear rates to bovine serum.

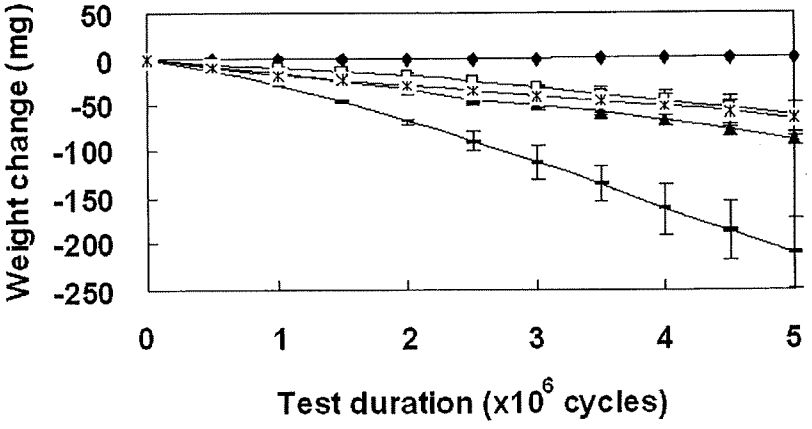


**Figure 2** Plot of cumulative weight loss of UHMWPE cups as a function of test duration for various lubricants: BSS (◆), BSS+A+G (□), BSS+1.5(A+G) (▲), CS1 (-) and CS2 (*).

Figure 3 shows SEM images of UHMWPE debris isolated from the various lubricants after 5.0 x $10^6$ cycles. No debris was observed in BSS (Fig. 3(a)). Elongated fibers were observed in BSS+A+G and BSS+1.5(A+G) (Figs. 3(b) and (c), respectively). Fibers and / or granules were observed in CS1 and CS2 (Figs. 3(d) and (e), respectively).

Table 2 shows the number and area of UHMWPE debris particles generated in the lubricants. The number and area of particles were significantly different among the lubricants. The number and area showed that particles generated in BSS tended to be most low value and those generated in CS1 were most high value, with intermediate values for the particles generated in

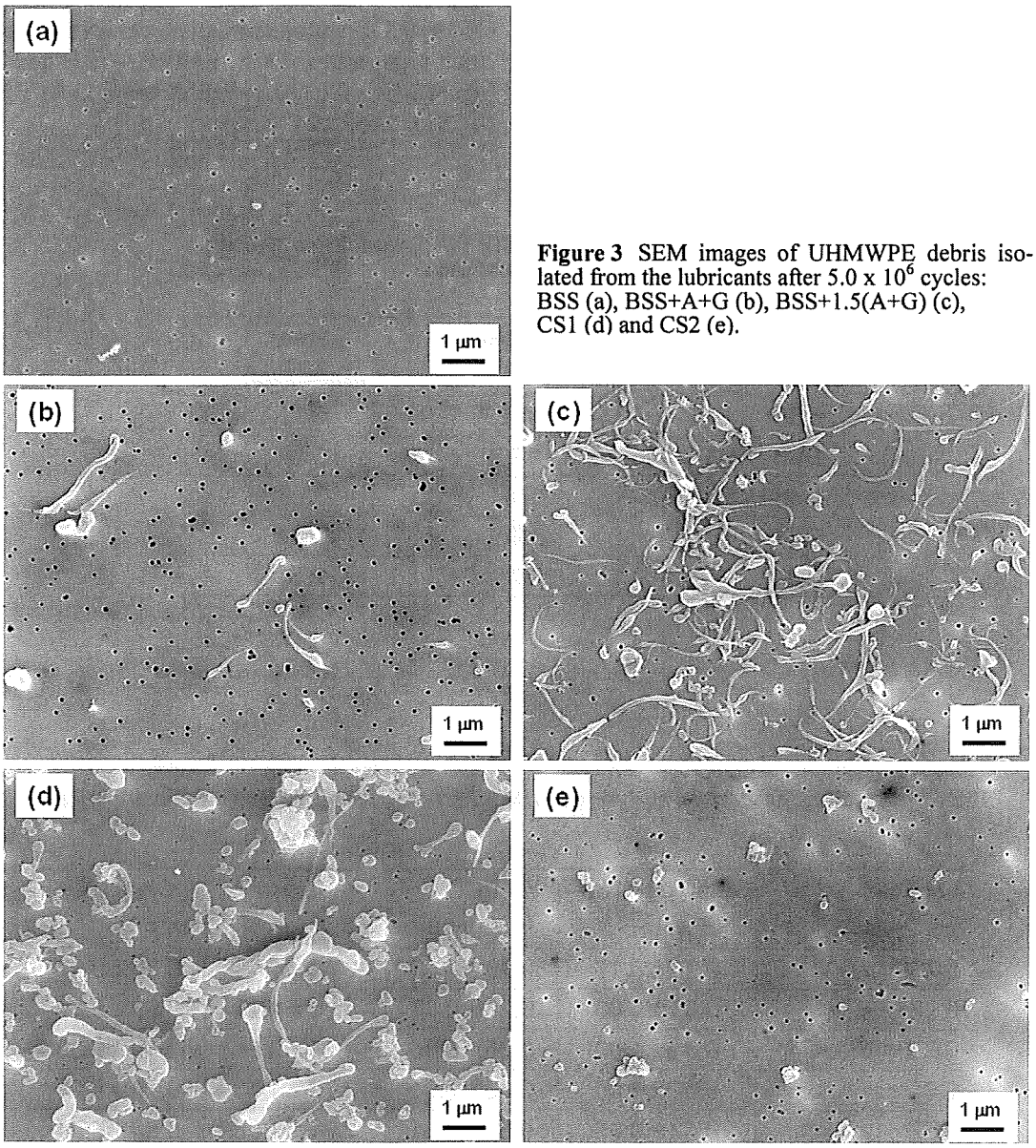


**Figure 3** SEM images of UHMWPE debris isolated from the lubricants after 5.0 x $10^6$ cycles: BSS (a), BSS+A+G (b), BSS+1.5(A+G) (c), CS1 (d) and CS2 (e).

BSS+A+G, BSS+1.5(A+G) and CS2. These results are consistent with the weight changes of the UHMWPE cups (Fig. 2).

The results of quantitative analysis of the UHMWPE wear debris generated in the lubricants are presented in Table 3 in the form of mean value ± standard error. The mean values of PS, ECD, AR and R were significantly different among the lubricants. It is apparent that the largest particles (mean PS: 0.89±1.40, mean ECD: 0.50±0.61) tended to be generated in CS1. The smallest particles (mean PS: 0.29±0.17, mean ECD: 0.16±0.07) were generated in BSS, with particles of intermediate sizes generated in BSS+A+G, BSS+1.5(A+G) and CS2. As might be expected, the values of mean AR indicate that elongated particles tended to be generated in BSS+A+G and BSS+1.5(A+G) (mean AR: 4.53±4.26 (BSS+A+G), 4.74±3.34 (BSS+1.5(A+G)). Particles generated in BSS, CS1 and CS2 tended to have lower ARs than those in BSS+A+G and BSS+1.5(A+G). The analysis of values of R showed that particles generated in BSS tended to be the most circular (mean R: 0.83±0.27) and those generated in BSS+1.5 (A+G) were the least circular (mean R: 0.49±0.33), with intermediate values for the particles generated in BSS+A+G, CS1 and CS2 (mean R: 0.63±0.34 (BSS+A+G), 0.70±0.29 (CS1), 0.66±0.24 (CS2)).

**Table 2** Number and area of UHMWPE wear debris particles generated in various lubricants.

| Lubricant | Number / ml | Area / ($\mu m^2$ / ml) |
|---|---|---|
| BSS | 1 | 0.02 |
| BSS+A+G | 17 | 2.06 |
| BSS+1.5(A+G) | 178 | 33.9 |
| CS1 | 362 | 175.6 |
| CS2 - | 77 | 16.6 |

**Table 3** Results of quantitative analysis of UHMWPE wear debris generated in various lubricants.

| Lubricant | Particle size / μm | ECD / μm | Aspect ratio | Circularity |
|---|---|---|---|---|
| BSS | 0.29±0.17 | 0.16±0.07 | 2.89±1.49 | 0.83±0.27 |
| BSS+A+G | 0.68±0.83 | 0.28±0.27 | 4.53±4.26 | 0.63±0.34 |
| BSS+1.5(A+G) | 0.81±1.00 | 0.35±0.35 | 4.74±3.34 | 0.49±0.33 |
| CS1 | 0.89±1.40 | 0.50±0.61 | 2.76±1.73 | 0.70±0.29 |
| CS2 | 0.52±0.65 | 0.31±0.31 | 2.71±1.08 | 0.66±0.24 |

All values expressed as mean±standard error.

Figure 4 shows the particle size distribution in the 0 – 20μm range for wear debris particles isolated from the lubricants. The distribution shows that the majority of particles removed from the surface were of 1 μm order in size. However, the particles isolated from CS1 and CS2 had a larger modal size than particles from BSS+A+G and BSS+1.5(A+G). For example, all of the particles isolated from BSS+A+G and BSS+1.5(A+G) were in the 0.5 – 5 μm size range, whereas those isolated from CS1 and CS2 were in the 0.5 – 17.5 μm size range.

Figure 5 shows the ECD distribution in the 0.5 – 7.5 μm range for the wear debris particles isolated from the lubricants. The distribution shows that the majority of particles removed from the surface had an ECD of less than 1 μm. However, the debris particles isolated from CS1 and CS2 had a considerably larger modal volume of ECD than that of particles from BSS+A+G and BSS+1.5(A+G). For instance, the ECD of particles isolated from BSS+A+G and BSS+1.5(A+G) was in the 0.5 – 2 μm range, whereas the ECD of particles isolated from CS1

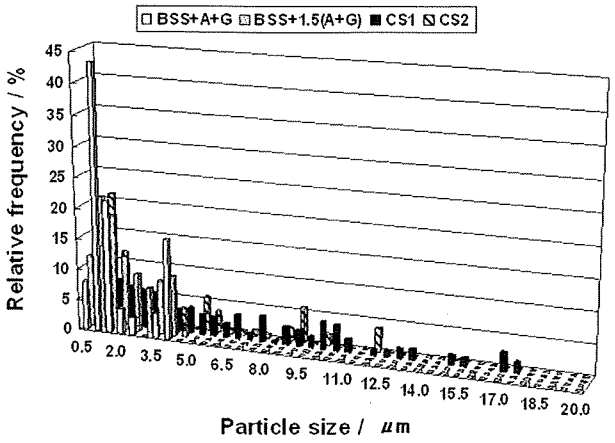


**Figure 4** Frequency distribution of size of UHMWPE debris particles isolated from various lubricants.

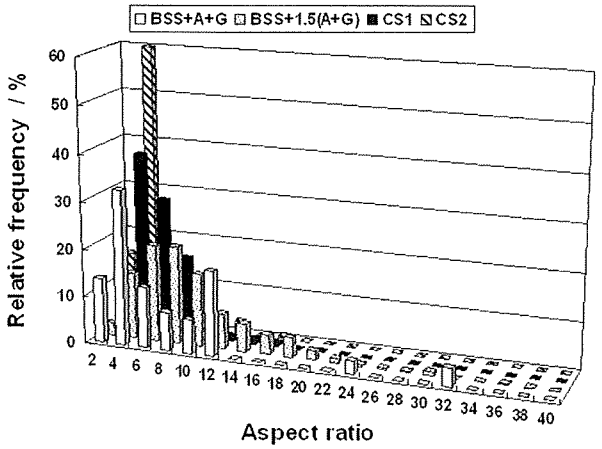


**Figure 6** Frequency distribution of aspect ratio of UHMWPE debris particles isolated from various lubricants.

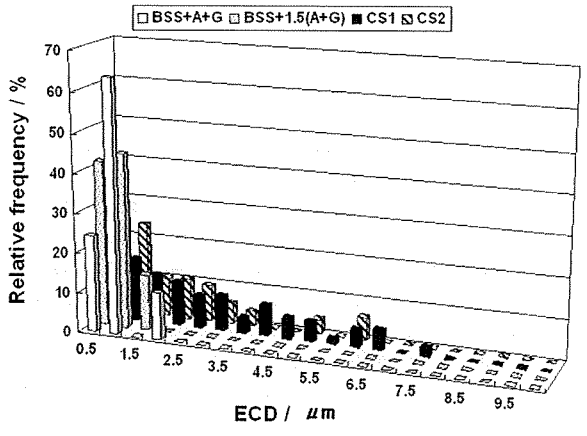


**Figure 5** Frequency distribution of ECD of UHMWPE debris particles isolated from various lubricants.

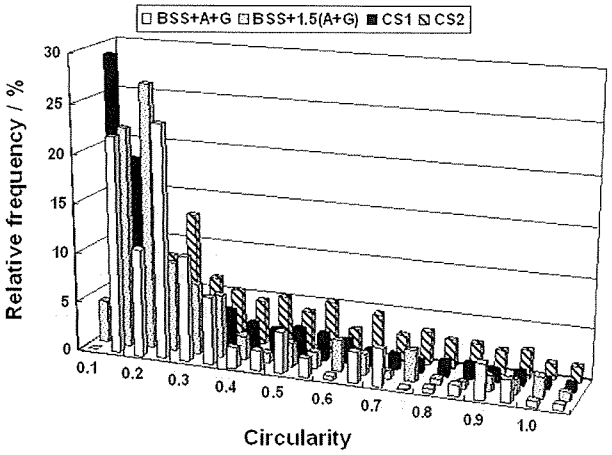


**Figure 7** Frequency distribution of circularity of UHMWPE debris particles isolated from various lubricants.

and CS2 was in the 0.5 – 7.5 μm range. The type of lubricant appeared to affect the particle size and ECD.

Figure 6 shows the aspect ratio distribution for the wear debris particles isolated from the lubricants. The distribution shows that the majority of particles removed from the surface had an aspect ratio of 4. The debris particles isolated from BSS+A+G and BSS+1.5(A+G) tended to have a higher aspect ratio than those isolated from CS1 and CS2. For instance, the aspect ratios of particles isolated from BSS+A+G and BSS+1.5(A+G) were in the 2 – 32 range, whereas those of particles isolated from CS1 and CS2 were in the 2 – 16 range.

Figure 7 shows the distribution of circularity for the wear debris particles isolated from the lubricants. The most frequently occurring value of circularity was within 0.1 – 0.2. About 80% of the particles isolated from BSS+1.5(A+G) had a circularity of 0.1 – 0.5, whereas those isolated from BSS+1.5(A+G), CS1 and CS2 mostly had a circularity of 0.1 – 0.4.

**Discussion**

In this study, a hip wear simulator was used to evaluate the wear of UHMWPE cups in various lubricants. Gravimetric wear rates and the quantitative measurements of wear debris were used in the evaluation. As expected, the weight loss due to the wear of the UHMWPE inserts increased with the number of test cycles, but the wear rate remained constant after a certain number of cycles, suggesting that a steady-state wear regime had been attained. However, the wear rate mainly depended on the total concentration of protein, irrespective of the type of lubricant (Fig. 2). The lubricant that produced the highest wear rate was BSS+1.5(A+G), which produced almost the same wear rate as CS1 up to the $1.0 \times 10^6$ th cycle, followed by BSS+A+G. Compared with these protein-containing lubricants, the protein-free lubricant (BSS) has very low friction. The wear rate from the first cycle up to the $1.0 \times 10^6$ th cycle (initial wear rate) remained relatively low but started to increase from the $4.0 \times 10^6$ th to $5.0 \times 10^6$ th cycle (steady wear rate).

The adsorption of albumin on prosthetic materials during contact with protein-containing solutions has been reported by several authors [13–15]. This albumin layer protects the surface of metals, zirconia and UHMWPE leading to the reduction of the friction coefficient to a low value. However, the albumin did not protect the surfaces of the alumina/UHMWPE coupling [16]. Norde *et al.* reported that the main components of the intermolecular forces responsible for protein adsorption are hydrophobic and electrostatic interactions [17]. In general, most proteins tend to be adsorbed more strongly on hydrophobic surfaces [18]. Furthermore, the adsorption of proteins that are able to undergo large conformational changes, the so-called soft proteins, is not generally dictated by electrostatic interactions [19]. The metal and zirconia have more hydrophobic surface than alumina. Also, in a simulation using a $ZrO_2$ head and a UHMWPE cup in bovine serum, the mean temperature increased to over 55 °C without forced cooling [20]. It is considered that the adsorbed albumin underwent large conformational changes under these conditions. Therefore, the adsorption of albumin protects the surfaces of the $ZrO_2$/UHMWPE hip joint.

In our studies, the $ZrO_2$/UHMWPE coupling was used in the hip simulator. The wear rate of UHMWPE against zirconia in this experiment increased, which was the same as that of UHMWPE against alumina. This was closely related to the experimental condition of hip simulator, as was observed *in vivo*. In fact, head and cup were completely immersed in a large amount of fluid (750 ml). On the other hand, temperature of this fluid was not controlled. These suggest that the presence of albumin in the lubricant did not avoid the adhesion and transfer of UHMWPE surface in our experiment.

The UHMWPE cup in CS1 exhibited a large weight loss throughout the wear testing, suggesting that it had been scored by third-body debris, possibly denatured protein particles from the serum. During the testing, particulates were precipitated in CS2. It is considered that the high protein concentration causes the proteins present in the lubricant to degrade and subsequently form proteinaceous precipitates. These precipitates cause an increase in UHMWPE wear and scratch the $ZrO_2$ counterface if they become trapped in the articulation.

The UHMWPE micron- and submicron-sized debris particles exhibited an inhomogeneous morphology that was consistent with previously proposed wear mechanisms. The determination of the wear mechanism from the particle morphology is complicated. Several primary wear mechanisms for hip cups have been proposed, including microasperity wear [21–24], microadhesive wear [21,

23] and residual subsurface strain [25, 26]. Fatigue and third-body wear may also be important secondary or tertiary mechanisms and may be responsible for the production of the larger particles.

Especially, two primary damage mechanisms, namely adhesive and abrasive wear, are commonly observed in surgically explanted UHMWPE components. Adhesive wear generally follows the orientation and strain hardening of the implant surface and subsequent implant motion results in the removal of small elongated wear particles, usually on the order of a few micrometers or less in size. Abrasive wear occurs through the rubbing action of the hard asperities on the surface of the femoral component. It is also accentuated by hard third body particles, such as bone chips or bone cement particles, within the articulation. Abrasive wear progresses by the cutting and removal of the polyethylene articular surface.

The appearance of elongated wear particles suggests that an adhesive mechanism, rather than the abrasive mechanism associated with asperities, was active [27]. The small submicron-sized granules may be the result of the comminution of the fibrils or may be an ultrastructural feature of the polymer [28]. In our studies, elongated wear particles with larger values of AR and smaller values of R were generated in BSS+A+G and BSS+1.5(A+G) (Table 3). The wear debris particles corresponding to BSS+A+G and BSS+1.5(A+G) were mainly of submicron size: 60% of the analyzed particles were in the 0.5 – 1.0 μm size ranges. Our results indicate that an adhesive wear mechanism occurred in BSS+A+G and BSS+1.5(A+G).

In conclusion, the results of our study suggest that the wear rate of a UHMWPE cup coupled to a $ZrO_2$ head depends on the total protein concentration. The wear rate decreased in the order CS1 > BSS+1.5(A+G) > CS2 > BSS+A+G > BSS $\simeq$ 0. The elongated wear particles generated in BSS+A+G and BSS+1.5(A+G) suggested that the adhesive wear mechanism was active, although a different wear mechanism was responsible for the wear in bovine sera (CS1 and CS2).

**Acknowledgments**

This work was supported in part by Health and Labor Science Research Grants provided by the Ministry of Health, Labor and Welfare of Japan to the Japan Fine Ceramics Center.

**References**

1) Affatato S, Bersaglia G, Emiliani D, Foltran I, Taddei P, Reggiani M, Ferrieri P, Toni A. The performance of gamma-and EtO-sterilised UHMWPE acetabular cups tested under severe simulator conditions. Part 2: wear particle characteristics with isolation protocols. Biomaterials 2003;24: 4045-4055
2) Wang A, Schmidig G. Ceramic femoral heads prevent runaway wear for highly crosslinked polyethylene acetabular cups by third-body bone cement particles. Wear 2003;255:1057-1063
3) Bragdon CR, Jasty M, Muratoglu OK, O'Connor DO, Harris WH. Third-body wear of highly cross-linked polyethylene in a hip simulator. J Arthroplasty 2003;18:553-561
4) Liao YS, McKellop H, Lu Z, Campbell P, Benya P. The effect of frictional heating and forced cooling on the serum lubricant and wear of UHMW polyethylene cups against cobalt-chromium and zirconia balls. Biomaterials 2003;24:3047-3059
5) Clarke IC, Chan FW, Essner A, Good V, Kaddick C, Lappalainen R, Laurent M, Mckellop H, McGarry W, Schroeder D, Selenius M, Shen MC, Ueno M, Wang A, Yao J. Multi-laboratory simulator studies on effects of serum proteins on PTFE cup wear. Wear 2001;250:188-198
6) Chandrasekaran M, Wei LY, Venkateshwaran KK, Batchelor AW, Loh NL. Tribology of UHMWPE tested against a stainless steel counterface in unidirectional sliding in presence of model synovial fluids: part 1.Wear 1998;223:13-21
7) Gispert MP, Serro AP, Colaco R, Saramago B. Friction and wear mechanisms in hip prosthesis: Comparison of joint materials behavior in several lubricants. Wear 2006;260:149-158
8) Shanbhag AS, Bailey HO, Hwang DS, Cha CW, Eror NG, Rubash HE. Quantitative analysis of ultrahigh molecular weight polyethylene (UHMWPE) wear debris associated with total knee replacements. J Biomed Mater Res Appl Biomater 2000;53:100-110
9) Calonius O, Saikko V. Analysis of polyethylene particles produced in different wear conditions in vitro. Clinical Orthopaedics and related research 2002;399:219-230
10) Takadama H, Hashimoto M, Mizuno M. Artificial lubricant solution analogous to bovine serum as a test medium for wear characterization of artificial hip joint, Proceeding of 10th International Conference and Exihibition of the European Ceramic Society, Berlin,Germany, 2007;17-21 June
11) Elfick APD, Smith SL, Green SM, Unsworth A. The quantitative assessment of UHMWPE wear debris produced in hip simulator testing: the influence of head ma-

terial and roughness, motion and loading. Wear 2001;249:517-527
12) McMullin BT, Leung MY, Shanbhag AS, McNulty D, Mabrey JD, Agrawal CM. Correlating subjective and objective descriptors of ultra high molecular weight wear particles from total joint prostheses. Biomaterials 2006;27:752-757
13) Urano H, Fukuzaki S. Influence of anionic compounds on adsorption behavior of bovine serum albumin at oxide-water interfaces. J Ferm Bioeng 1997;83:261-266
14) Williams RL, Williams DF. The effect of albumin on the wettability of pure metal and metal surfaces. J. Colloid Interface Sci. 1988;126:596-603
15) Fukusaki S, Urano H, Nagata K. Adsorption of protein onto stainless-steel surfaces. J Ferm Bioeng 1995;80:6-11
16) Urano H, Fukusaki S. Conformation of adsorbed bovine serum albumin governing its desorption behavior at alumina/water interfaces. J Biosci Bioeng 2000;99:105-111
17) Haynes C, Norde W. Globular proteins at solid/liquid interfaces. Colloid Surf B: Biointerfaces. 1994;2:517-566
18) Norde W, Haynes C. Thermodynamics of protein adsorption, in: J. L. Brash, P. Wojciechowski (Eds), Interfacial Phenomena and Bioproducts, Marcel Dekker, New York, 1996, pp. 122-144
19) Malmsten M. Formation of adsorbed protein layers. J Colloid Interface Sci 1998;207: 186-199
20) Liao YS, McKellop H, Lu Z, Campbell P, Benya P. The effect of frictional heating and forced cooling on the serum lubricant and wear of UHMW polyethylene cups against cobalt-chromium and zirconia balls. Biomaterials. 2003;24:3047-3059
21) Mckellop HA, Campbell P, Park SH. The origin of submicron polyethylene wear debris in total hip arthroplasty. Clin Orthop Rel Res 1995;311:3-20
22) Cooper JR, Dowson D, Fisher J. The effect of transfer film and surface roughness on the wear of lubricated ultra-high molecular weight polyethylene. Clin Mater 1993;14: 295-302
23) Davidson JA. Characteristics of metal, ceramic total hip bearing surafces and their effect on long-term ultra-high molecular weight polyethylene wear. Clin Orthop Relat Res 1993;294:361-378
24) Fisher J, Chan KL, Hailey JL, Shaw D, Stone M. Preliminary study of the effect of aging following irradiation on the wear of ultrahigh-molecular-weight polyethylene. J Arthroplasty. 1995;10:689-692
25) Fisher J, Copper J, Dowson D, Isaac G, Wroblewski B. 1993. Wear mechanisms and sub-surface failure in UHMWPE acetabular cups. In: Proceedings of the 39th Annual Meeting of the Orthopaedic Research Society. USA, San Francisco, pp.509
26) Mcdonald MD, Bloebaum RD. Distinguishing wear and creep in clinically retrieved polyethylene inserts. J. Biomed Mater Res 1995;29:1-7
27) Campbell P, Dorey F, Amstutz AC. Wear and morphology of ultra-high-molecular-weight-polyethylene wear particles from total hip replacements. Proc Inst Mech Eng Part H. 1996;210:167-174
28) Pienkowski D, Jacob R, Hoglin D, Saum K, Kaufer H, Nicholls PJ. Low-voltage scanning electron microscopic imaging of ultra-high-molecular-weight polyethylene. J Biomed Mater Res. 1995;29:1167-1174

(Received: May 27/
Accepted: Jun 10)

**Corresponding author:**
Dr. Masami HASHIMOTO
Japan Fine Ceramics Center
2-4-1 Mutsuno, Atsuta-ku,
Nagoya, 456-8587 Japan
Tel. +81-52-871-3500
Fax +81-52-871-3599
E-mail: masami@jfcc.or.jp

Biomaterials 31 (2010) 1017–1024

Contents lists available at ScienceDirect

Biomaterials

journal homepage: www.elsevier.com/locate/biomaterials

# Self-initiated surface grafting with poly(2-methacryloyloxyethyl phosphorylcholine) on poly(ether-ether-ketone)

Masayuki Kyomoto [a,b,e], Toru Moro [b,c], Yoshio Takatori [b,c], Hiroshi Kawaguchi [c], Kozo Nakamura [c], Kazuhiko Ishihara [a,d,*]

[a] Department of Materials Engineering, School of Engineering, The University of Tokyo, 7-3-1, Hongo, Bunkyo-ku, Tokyo 113-8656, Japan
[b] Division of Science for Joint Reconstruction, Graduate School of Medicine, The University of Tokyo, 7-3-1, Hongo, Bunkyo-ku, Tokyo 113-8655, Japan
[c] Sensory & Motor System Medicine, Faculty of Medicine, The University of Tokyo, 7-3-1, Hongo, Bunkyo-ku, Tokyo 113-8655, Japan
[d] Center for NanoBio Integration, The University of Tokyo, 7-3-1, Hongo, Bunkyo-ku, Tokyo 113-8656, Japan
[e] Research Department, Japan Medical Materials Corporation, 3-3-31, Miyahara, Yodogawa-ku, Osaka 532-0003, Japan

ARTICLE INFO

*Article history:*
Received 20 August 2009
Accepted 25 October 2009
Available online 10 November 2009

*Keywords:*
Polyetheretherketone
Phosphorylcholine
Surface modification
Photopolymerization
Protein adsorption
Friction

ABSTRACT

Poly(ether-ether-ketone) (PEEK)s are a group of polymeric biomaterials with excellent mechanical properties and chemical stability. In the present study, we demonstrate the fabrication of an antibiofouling and highly hydrophilic high-density nanometer-scaled layer on the surface of PEEK by photo-induced graft polymerization of 2-methacryloyloxyethyl phosphorylcholine (MPC) without using any photo-initiators, i.e., "self-initiated surface graft polymerization." Our results indicated that the diphenylketone moiety in the polymer backbone acted as a photo-initiator similar to benzophenone. The density and thickness of the poly(MPC) (PMPC)-grafted layer were controlled by the photo-irradiation time and monomer concentration during polymerization, respectively. Since MPC is a highly hydrophilic compound, the water wettability (contact angle $<10^{\circ}$) and lubricity (coefficient of dynamic friction $<0.01$) of the PMPC-grafted PEEK surface were considerably lower than those of the untreated PEEK surface ($90^{\circ}$ and 0.20, respectively) due to the formation of a PMPC nanometer-scale layer. In addition, the amount (0.05 $\mu g/cm^2$) of BSA adsorbed on the PMPC-grafted PEEK surface was considerably lower, that is more than 90% reduction, compared to that (0.55 $\mu g/cm^2$) for untreated PEEK. This photo-induced polymerization process occurs only on the surface of the PEEK substrate; therefore, the desirable mechanical properties of PEEK would be maintained irrespective of the treatment used.



## 1. Introduction

Poly(aryl-ether-ketone) (PAEK), including poly(ether-ether-ketone) (PEEK), is a new family of high performance thermoplastic polymers, consisting of an aromatic backbone molecular chain interconnected by ketone and ether functional groups, i.e., a benzophenone (BP) unit is included in its molecular structure. Polyaromatic ketones exhibit enhanced mechanical properties, and their chemical structure is stable, resistant to chemical and radiation damage, and compatible with several reinforcing agents (such as glass and carbon fibers); therefore, they are considered to be promising materials for not only industrial applications but also biomedical applications. In the 1980s, the *in vivo* stability of various PAEK materials and the tissue response to those were investigated [1]. Recently, PEEK has emerged as the leading high-performance super-engineering plastic candidate for replacing metal implant components, especially in the field of orthopedics and spinal surgery [2]. In recent studies, the tribological and bioactive properties of PEEK, which is used as a bearing material and flexible implant in orthopedic and spinal surgeries, has been investigated [3–5]. However, conventional single-component PEEK cannot satisfy these requirements (e.g., antibiofouling, wear resistance, and fixation to a bone) for use as an artificial joint or intervertebral body fusion cage [2]. For further improving the capabilities of PEEK as an implant biomaterial, various studies have focused upon the lubricity and antibiofouling of the polymer, either via reinforcing agents or surface modifications [6,7]. Therefore, multicomponent polymer systems have been designed in order to synthesize new multifunctional biomaterials. In order to use PEEK and related composites in the implant applications, they can be engineered to have a wide range of physical, mechanical, and surface properties.

* Corresponding author. Department of Materials Engineering, School of Engineering, The University of Tokyo, Hongo 7-3-1, Bunkyo-ku, Tokyo 113-8656, Japan. Tel.: +81 3 5841 7124; fax: +81 3 5841 8647.
*E-mail address:* ishihara@mpc.t.u-tokyo.ac.jp (K. Ishihara).

0142-9612/$ – see front matter © 2009 Elsevier Ltd. All rights reserved.
doi:10.1016/j.biomaterials.2009.10.055

Surface modification is one of the most important technologies for the preparation of new multifunctional biomaterials for satisfying several requirements; surface modifications used today include coating, blending, and grafting. In general, graft polymerization is performed most frequently using either of the following methods that utilize chemical and/or physical processes: (a) surface-initiated graft polymerization or "grafting from" methods in which the monomers are polymerized from initiators or comonomers, and (b) adsorption of the polymer to the substrate or "grafting to" methods, such as reaction of the end groups of the ready-made polymers with the functional groups of the substrate. The "grafting from" method has an advantage over the "grafting to" method wherein it forms a high-density polymer brush interface with a multifunctional polymer; this advantage proves to be functionally effective.

It is well known that when BP is exposed to photo-irradiation such as ultraviolet-ray (UV)-irradiation, a pinacolization reaction is induced; this results in the formation of semi-benzopinacol radicals (i.e., ketyl radicals) that act as photo-initiators. Therefore, in this study, we have focused upon a BP unit in PEEK and formulated a self-initiated surface-graft polymerization method that utilizes the BP unit in graft-from polymerization (Fig. 1) [8]. This polymerization reaction involving free radicals is photo-induced by UV-irradiation. Under UV-irradiation, a BP unit in PEEK can undergo the following reactions in the monomer aqueous solutions [9–15]: the pinacolization reaction (photo-reduction by the H-abstraction of a BP unit in PEEK) results in the formation of a semi-benzopinacol radical, which can initiate the graft-from polymerization of the feed monomer as the main reaction, and the graft-to polymerization (the radical chain end of the active-polymer couples with the semi-benzopinacol radical of the PEEK surface) as a sub-reaction. In addition, a photo-scission reaction occurs as a sub-reaction, which may not need an hydrogen (H)-donor. The cleavage reaction induces recombination and the graft-from polymerization. When water polymerization is performed in the presence of an H-donor, a phenol unit may be sub-sequentially formed due to H-abstraction. This technique enables the direct grafting of the functional polymer onto the PEEK surface in the absence of a photo-initiator, thereby resulting in the formation of a C–C covalent bond between the functional polymer and PEEK substrate.

2-Methacryloyloxyethyl phosphorylcholine (MPC), a methacrylate monomer bearing a phosphorylcholine group, is used to synthesize polymer biomaterials having excellent biocompatibility [16–25]; the MPC polymers have potential applications in a variety of fields such as biomedical science, surface science, and bioengineering because they possess unique properties such as excellent antibiofouling, and low friction abilities. Thus, surface modification with the MPC polymer on medical devices is effective for obtaining biocompatibility. Several medical devices have already been developed by utilizing MPC polymers and have been used clinically; therefore, the efficacy and safety of MPC polymers as biomaterials are well-established [23–25].

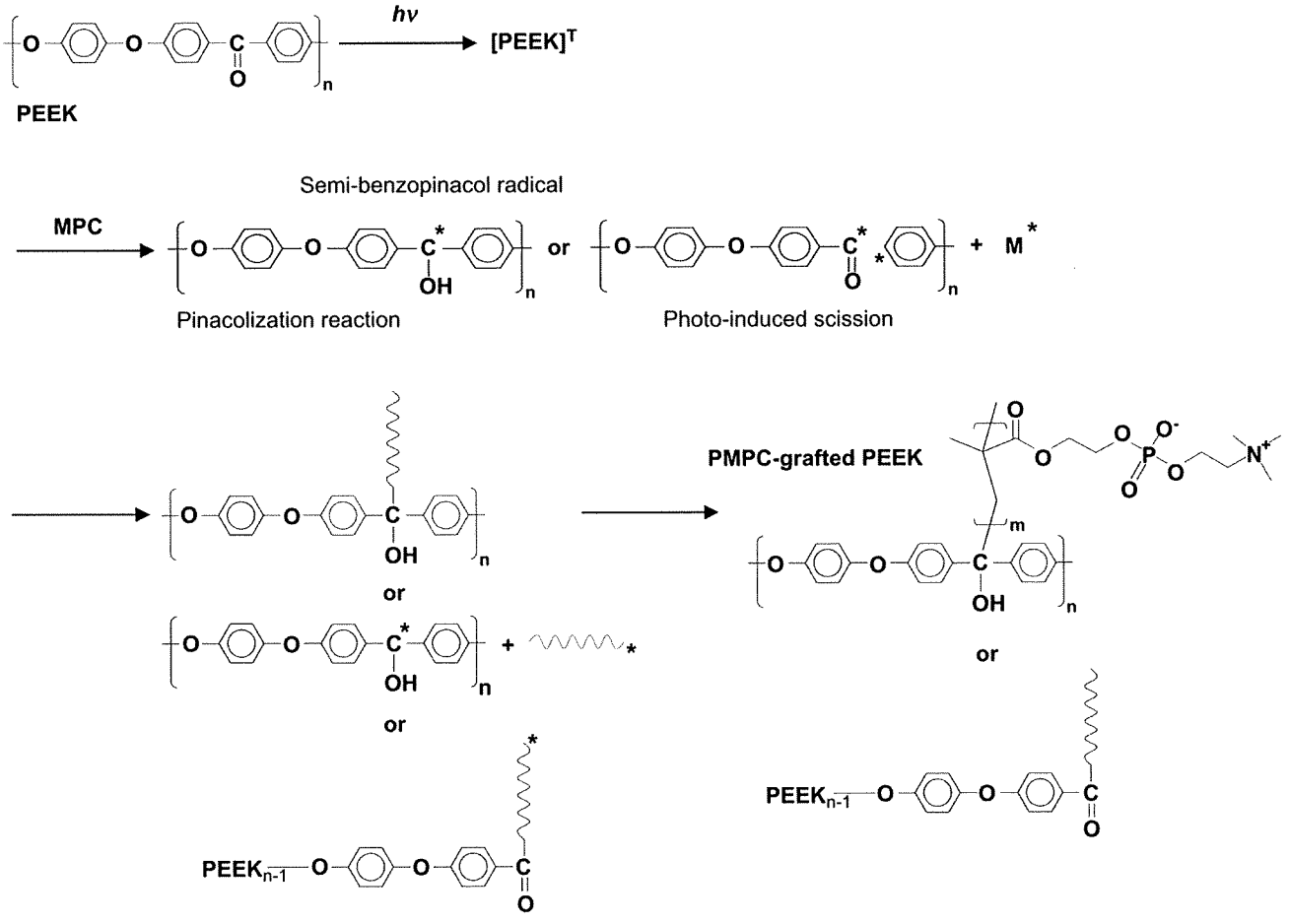


**Fig. 1.** Schematic illustration for the preparation of PMPC-grafted PEEK.

In this study, we have demonstrated the fabrication of a biocompatible and highly hydrophilic nanometer-scale-modified surface by poly(MPC) (PMPC)-grafting onto the self-initiated PEEK surface using a photo-induced pinacolization reaction; further, we also investigated the effects of photo-irradiation time and MPC concentration variability on PMPC-graft polymerization. The results revealed that it was possible to control the PMPC-graft layer in order to improve wettability, lubricity, and anti-protein adsorption for developing multifunctional PEEK biomaterials.

## 2. Materials and methods

### 2.1. Self-initiated graft polymerization of MPC

The preparation of PMPC-grafted PEEK is schematically illustrated in Fig. 1. PEEK specimens were machined from an extruded PEEK (450 G; Victrex PLC, Thornton-Cleveleys, UK) bar stock, which was fabricated without stabilizers or additives. The surfaces of the PEEK specimens were ultrasonically cleaned in ethanol for 20 min, and then dried in vacuum. MPC was industrially synthesized using the method reported by Ishihara et al. [26] and supplied by NOF Corp. (Tokyo, Japan). It was dissolved in degassed water to obtain 0.25- and 0.50-mol/L MPC aqueous solutions, and PEEK specimens were immersed in these solutions. Photo-induced graft polymerization was carried out at 60 °C for 5–90 min on the PEEK surface under UV-irradiation (UVL-400HA ultra-high pressure mercury lamp; Riko-Kagaku Sangyo Co. Ltd., Funabashi, Japan) with an intensity of 5 mW/cm$^2$; a filter (model D-35; Toshiba Corp., Tokyo, Japan) was used to restrict the passage of UV-light to wavelengths of 350 ± 50 nm. After polymerization, the PMPC-grafted PEEK specimens were removed from the reaction solution, washed with pure water and ethanol to remove non-reacted monomers and non-grafted polymers, and dried at room temperature.

### 2.2. Surface analysis of PMPC-grafted PEEK

The functional group vibrations of the PMPC-grafted PEEK surfaces were examined by Fourier-transform infrared (FT-IR) spectroscopy with attenuated total reflection (ATR) equipment. The FT-IR/ATR spectra were obtained using an FT-IR analyzer (FT/IR615; JASCO Co. Ltd., Tokyo, Japan) for 32 scans over the range of 1000–1800 cm$^{-1}$ at a resolution of 4.0 cm$^{-1}$.

The surface elemental conditions of the PMPC-grafted PEEK surfaces were analyzed by X-ray photoelectron spectroscopy (XPS). The XPS spectra were obtained using an XPS spectrophotometer (AXIS-HSi165; Kratos/Shimadzu Co., Kyoto, Japan) equipped with a 15-kV Mg-$K_\alpha$ radiation source at the anode. The take-off angle of the photoelectrons was maintained at 90°. Five scans were taken for each sample.

The static-water contact angles on the PMPC-grafted PEEK surfaces were measured by the sessile drop method using an optical bench-type contact angle goniometer (Model DM300; Kyowa Interface Science Co. Ltd., Saitama, Japan). Drops of purified water (1.0 μL) were deposited on the PMPC-grafted PEEK surfaces, and the contact angles were directly measured with a microscope after 60 s of dropping. Measurements were repeated fifteen times for each sample, and the average values were regarded as the contact angles.

### 2.3. Cross-sectional observation by transmission electron microscopy

A cross-section of the PMPC layer on the PMPC-grafted PEEK surface was observed using a transmission electron microscope (TEM). The specimens were first embedded in epoxy resin, stained with ruthenium oxide vapor at room temperature, and then sliced into ultra-thin films (approximately 100-nm thick) by using a Leica Ultra Cut UC microtome (Leica Microsystems, Ltd., Wetzlar, Germany). A JEM-1010 electron microscope (JEOL, Ltd., Tokyo, Japan) was used for the TEM observation at an acceleration voltage of 100 kV. The thickness of the PMPC layer was determined by averaging ten points on the cross-sectional TEM image.

### 2.4. Gravimetric measurement of PMPC-grafted layer

The PMPC-grafted PEEK specimens were weighed on a microbalance (Sartorius Supermicro S4; Sartorius AG, Goettingen, Germany) to determine the physical properties of the PMPC-grafted layer. The physical properties were obtained by the following equations:

$$\text{PMPC} - \text{graftextent}(\text{g/cm}^2) = (W_g - W_0)/S \quad (1)$$

$$\text{PMPC} - \text{graftlayerdensity}(\text{g/cm}^3) = (W_g - W_0)/S \times T \quad (2)$$

where $W_0$ is the initial weight of the untreated PEEK substrate, $W_g$ is the weight of the PMPC-grafted PEEK in dry condition, $S$ is the grafted surface area of the PEEK substrate, and $T$ is the thickness of the PMPC-graft layer determined by cross-sectional TEM observation. The weighing was repeated five times for each sample, and the average values were regarded as the weight of the samples.

### 2.5. Characterization of protein adsorption by micro-bicinchoninic acid method

The amount of protein adsorbed on the PMPC-grafted PEEK surfaces was measured by the micro-bicinchoninic acid (BCA) method. Each specimen was immersed in Dulbecco's phosphate-buffered saline (PBS, pH 7.4, ion strength = 0.15 M; Immuno-Biological Laboratories Co. Ltd., Takasaki, Japan) for 1 h to equilibrate the PMPC-grafted surface. The specimens were immersed in bovine serum albumin (BSA, $M_w = 6.7 \times 10^4$; Sigma-Aldrich Corp., MO, USA) solution at 37 °C for 1 h. The protein solution was prepared in a BSA concentration of 4.5 g/L, i.e., 10% of the concentration of human plasma levels. Then, the specimens were rinsed five times with fresh PBS and immersed in 10.0 g/L sodium dodecyl sulfate (SDS) aqueous solution and shaken at room temperature for 1 h to completely detach the adsorbed BSA on the PMPC-grafted surface. A protein analysis kit (micro BCA protein assay kit, #23235; Thermo Fisher Scientific Inc., IL, USA) based on the BCA method was used to determine the BSA concentration in the SDS solution, and the amount of BSA adsorbed on the PMPC-grafted PEEK surface was calculated.

### 2.6. Friction test

The friction test was performed using a pin-on-plate machine (Tribostation 32; Shinto Scientific Co. Ltd., Tokyo, Japan). Each of the PMPC-grafted PEEK surfaces was used to prepare five sample pieces. A 9-mm-diameter pin with Co-Cr-Mo alloy was prepared. The surface roughness ($R_a$) of the pin was <0.01, which was comparable to that of femoral head products. The friction tests were performed at room temperature with a load of 0.98 N, sliding distance of 25 mm, and a frequency of 1 Hz for a maximum of 100 cycles. Pure water was used as a lubricant. The mean coefficients of dynamic friction were determined by averaging five data points from the 100 (96–100) cycle measurements.

### 2.7. Mechanical test

The mechanical properties of untreated PEEK and PMPC-grafted PEEK with a 0.50-mol/L MPC concentration and 90-min photo-irradiation time were evaluated with tensile and flexural tests. Tensile testing was performed according to ISO527 standard using a type 1B tensile bar specimen and a crosshead speed of 50 mm/min. Flexural testing was performed according to ISO178 standard with a crosshead speed of 2 mm/min. The results derived from each measurement in the mechanical test were expressed as the mean values ± standard deviation. The statistical significance ($p < 0.05$) was estimated by Student's $t$-test.

## 3. Results

Fig. 2 shows the FT-IR/ATR and XPS spectra of untreated PEEK and PMPC-grafted PEEK with a 0.50-mol/L MPC concentration and 90-min photo-irradiation time. Transmission absorption peaks were observed at 1600, 1490, 1280, 1190, and 1160 cm$^{-1}$ for both untreated PEEK and PMPC-grafted PEEK (Fig. 2(A)). These peaks are chiefly attributed to the diphenyl ether group, phenyl rings, or aromatic hydrogens in the PEEK substrate [8,27]. However, absorption peaks at 1720 and 1080 cm$^{-1}$ (shoulder peak) were observed only for PMPC-grafted PEEK. These peaks corresponded to the carbonyl group (C=O) and phosphate group (P–O) in the MPC unit, respectively [8,25]. The XPS spectra of the binding energy region of the nitrogen (N) and phosphorous (P) electrons showed peaks for untreated PEEK and PMPC-grafted PEEK, whereas, peaks were not observed in the case of untreated PEEK (Fig. 2(B)). The peaks at 403 and 134 eV were attributed to the $-N^+(CH_3)_3$ and phosphate groups, respectively. These peaks indicate the presence of phosphorylcholine in the MPC units. After PMPC-grafting, the peaks attributed to the MPC unit were clearly observed in both the FT-IR/ATR and XPS spectra of the PMPC-grafted PEEK. These results indicate that PMPC was successfully grafted on the PEEK surface [8,25].

Fig. 3 shows the N and P concentrations of the PMPC-grafted PEEK as a function of the photo-irradiation time during polymerization at 0.25- and 0.50-mol/L MPC concentrations. The N and P concentrations increased with the photo-irradiation time. When the photo-irradiation time was shorter than 45 min, the N and P concentrations of the PMPC-grafted PEEK surface with a 0.50-mol/L MPC concentration were higher as compared with those with a 0.25-mol/L MPC concentration. The N and P concentration in the PMPC-grafted PEEK with both 0.25- and 0.50-mol/L MPC

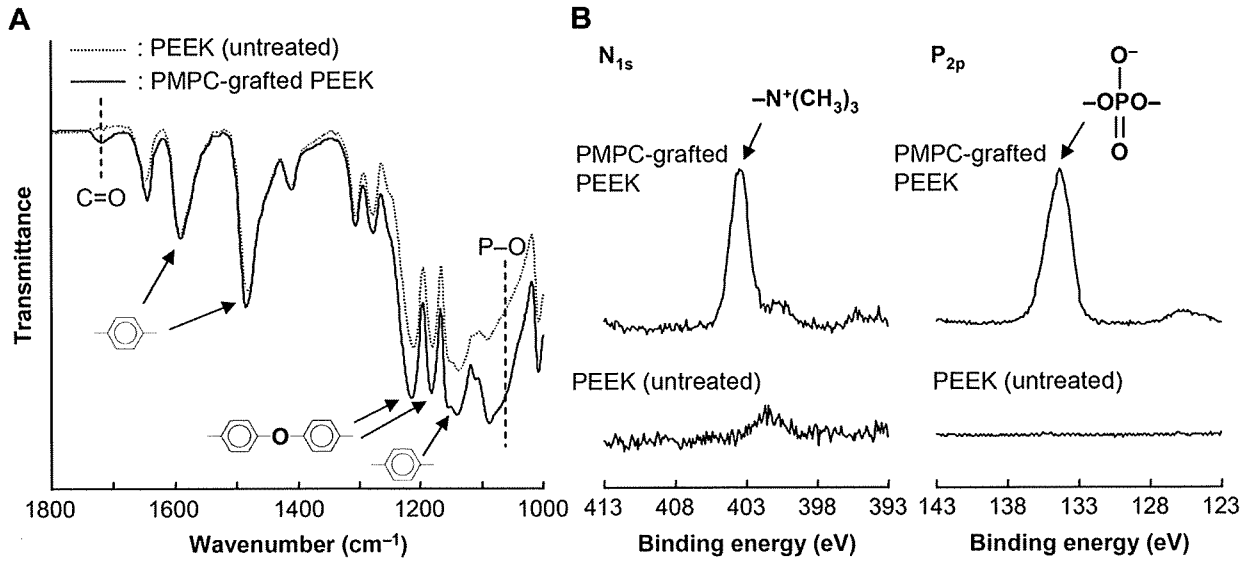


**Fig. 2.** FT-IR/ATR (A) and XPS (B) spectra of untreated and PMPC-grafted PEEK.

concentrations increased to 5.2 up to a photo-irradiation time of 90 min; those values were almost equivalent to the theoretical elemental composition (N = 5.3, P = 5.3) of PMPC. These results indicate that the PMPC layer fully covered the surface of the PEEK substrate.

Fig. 4 shows the cross-sectional TEM images of PMPC-grafted PEEK obtained with a 0.50-mol/L concentration and various photo-irradiation times as well as the PMPC-graft layer thickness determined by the TEM observations. With photo-irradiation times longer than 45 min, a uniform PMPC layer was clearly observed on the PEEK surface (Fig. 4(A)). The PMPC-graft layer thickness increased with the photo-irradiation time (Fig. 4(B)). In the case of both 0.25- and 0.50-mol/L MPC concentrations, when the photo-irradiation time was greater than 45 min, the PMPC-graft layer thicknesses became almost constant at 40 and 100, respectively.

Fig. 5 shows the physical properties of PMPC-graft layer on the PEEK surface as a function of the photo-irradiation time at MPC concentrations of 0.25 and 0.50 mol/L. The PMPC-graft extent of the PMPC-grafted PEEK with both 0.25- and 0.50-mol/L MPC concentration increased gradually with the photo-irradiation time (Fig. 5(A)). The PMPC-graft layer density of the PMPC-grafted PEEK with 0.25-mol/L MPC concentration increased proportionally to 2.3 g/cm$^3$ with the photo-irradiation time. In the case of PMPC-grafted PEEK obtained with 0.50-mol/L MPC concentration, the PMPC-graft layer density rapidly increased to 1.3 g/cm$^3$ up to a photo-irradiation time of 10 min; it then increased slowly to 2.2 g/cm$^3$ with an increase in the photo-irradiation time.

Fig. 6 shows the static-water contact angle of PMPC-grafted PEEK obtained with MPC concentrations of 0.25 and 0.50 mol/L as a function of the photo-irradiation time. The static-water contact angle of untreated PEEK was 90° and decreased markedly with an increase in the photo-irradiation time. When the photo-irradiation time was 90 min, the static-water contact angle of PMPC-grafted PEEK was the lowest value at <10°.

Fig. 7 shows the coefficient of dynamic friction of PMPC-grafted PEEK obtained with 0.25- and 0.50-mol/L MPC concentrations and various photo-irradiation times. For PMPC-grafted PEEK obtained with both 0.25- and 0.50-mol/L MPC concentrations, these coefficients of dynamic friction decreased markedly with an increase in photo-irradiation time. The PMPC-grafted PEEK obtained with 90 min photo-irradiation time was the lowest at <0.01, and exhibited approximately 95% reduction in their coefficients of dynamic friction when compared with the untreated PEEK.

Fig. 8 shows the amount of adsorbed BSA of PMPC-grafted PEEK as a function of the photo-irradiation time with MPC concentrations of 0.25 mol/L and 0.50 mol/L. The amount of adsorbed BSA of PMPC-grafted PEEK decreased remarkably with an increase in photo-irradiation time.

The mechanical properties of untreated PEEK and PMPC-grafted PEEK are summarized in Table 1. Tensile properties and flexural modulus did not differ significantly ($p > 0.05$) between untreated PEEK and PMPC-grafted PEEK. In contrast, there was a small but significant difference ($p < 0.05$) in the flexural strength and strain of untreated PEEK and PMPC-grafted PEEK examined in this study. However, both untreated PEEK and PMPC-grafted PEEK met the ASTM F2026 requirements [28].

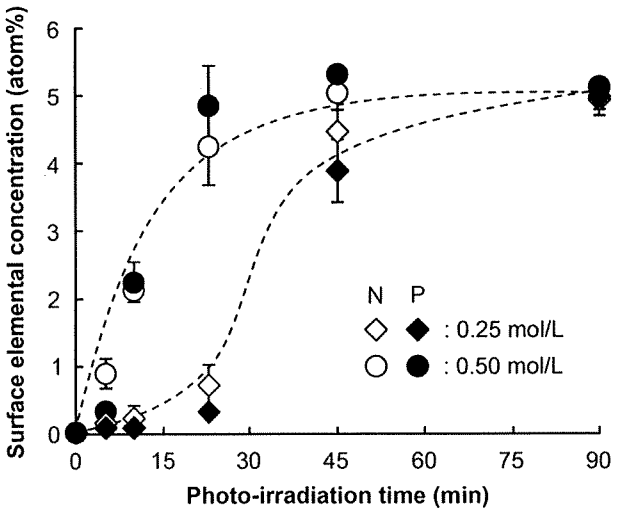


**Fig. 3.** Surface elemental concentration ($n = 5$) of PMPC-grafted PEEK as a function of the photo-irradiation time with MPC concentrations of 0.25 and 0.50 mol/L. Bar: Standard deviation.

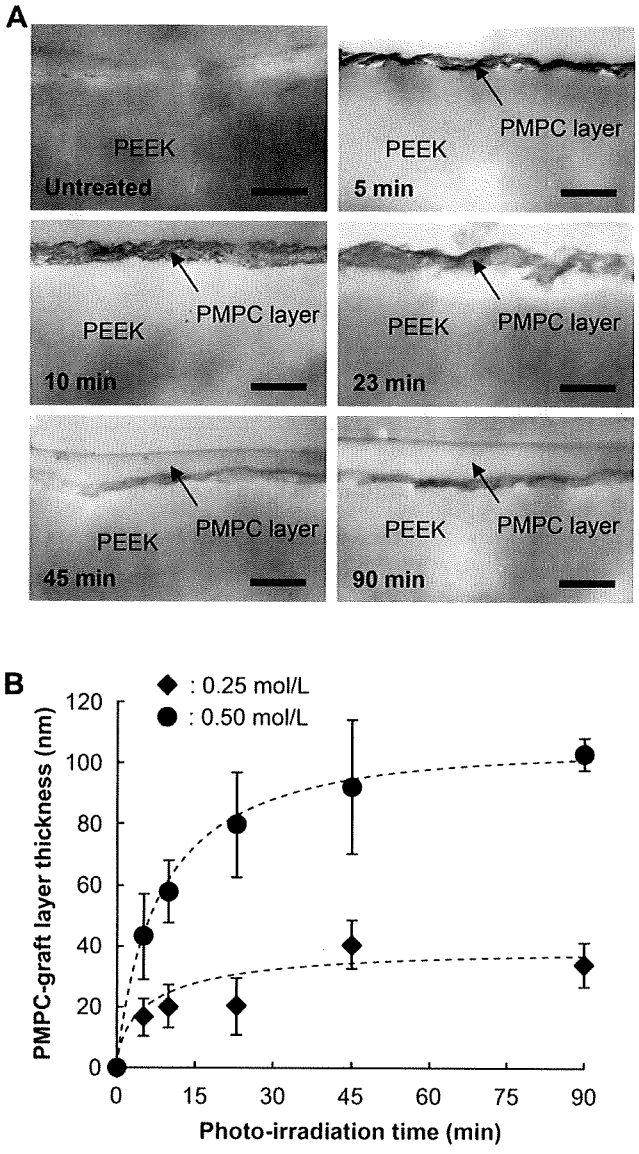


**Fig. 4.** Cross-section of the PMPC-grafted PEEK. (A) Cross-sectional TEM images of PMPC-grafted PEEK obtained with a MPC concentration of 0.5 mol/L and various photo-irradiation times. Bar: 100 nm. (B) PMPC-graft layer thickness ($n = 10$) determined by TEM observation. Bar: Standard deviation.

## 4. Discussion

In this study, we demonstrated the fabrication of a biocompatible and highly hydrophilic nanometer-scale-modified surface by PMPC-grafting onto the self-initiated PEEK surface using a photo-induced grafting-from polymerization reaction, i.e., "self-initiated surface graft polymerization." The following methods were employed in our study: (a) grafting from polymerization for the formation of a high-density graft polymer layer, (b) photo-induced polymerization in the absence of photo-initiators, and (c) using biocompatible hydrophilic macromolecules, which exhibited photo-reduction by H-abstraction of a BP unit in PEEK from an H-donor; this induced surface-initiated graft polymerization of the feed methacrylate-type monomer (i.e., MPC) on the PEEK surface, even in the absence of a photo-initiator such as BP. This report discusses the structure of the PMPC layer of PMPC-grafted PEEK in terms of the condition variability of self-initiated surface graft polymerization and its effects on antibiofouling and hydrophilicity.

It is important to control the graft layer thickness and density for optimizing several areas of applications, e.g., in adhesion, colloid stabilization, and lubrication. In Fig. 4, when the photo-irradiation time was greater than 45 min, the PMPC-graft layer thicknesses became almost constant. Moreover, at the same photo-irradiation time of 90 min, it was shown that the higher the monomer concentration, the thicker the graft layer obtained: the PMPC-graft layer thickness (approximately 100 nm) of the PMPC-grafted PEEK obtained with 0.50-mol/L MPC concentration was thicker than that (approximately 40 nm) with 0.25-mol/L MPC concentration. The phenomenon can be attributed to the fact that the graft layer thickness increases with monomer concentration. When the PMPC layer has a brush-like structure, the graft layer thickness may correlate with the molecular weight of the grafted PMPC. The high-density PMPC-graft layer on the PEEK surface is assumed to exhibit a brush-like structure [29,30]. It is generally well known that the reaction rate of radical polymerization is extremely high [31]. It was observed that the graft layer thickness (i.e., molecular weight of the graft polymer) was greatly dependent on the monomer concentration, but virtually independent of the photo-irradiation time. Thus, in this study, the length (molecular weight) of the PMPC-graft chains was assumed to be successfully controlled by the MPC concentration used for polymerization. This indicates that the length of the PMPC chain grafted on the PEEK surface increased with the MPC concentration during polymerization [32]. Additionally, a uniform PMPC layer was clearly observed on the surface of the PEEK substrate, and no cracks or delamination were observed at the PEEK substrate or the interface between the PMPC layer and PEEK substrate. These results indicate that the PMPC layer formed on the PEEK substrate is uniformly distributed over the substrate and is bound to the substrate by covalent C–C bonds.

On the other hand, the PMPC-graft layer density on the PEEK surface almost linearly increased to >2.2 g/cm$^3$ with the photo-irradiation time, suggesting that the graft chain propagates steadily with increasing photo-irradiation time (Fig. 5(B)). In order to obtain the high-density PMPC-graft layer, the photo-irradiation time must be controlled. Further, interestingly, while using an MPC concentration of 0.50 mol/L, the rate of the increase in the PMPC-graft layer density was low with a photo-irradiation time above 10 min. The present self-initiated surface graft polymerization method is photo-induced by UV-irradiation onto the BP unit of PEEK surface. In this study, it is assumed that the UV-irradiation directly produces a high-concentration free radical, because this PEEK is a semi-crystalline structure (crystallinity, 30–40%) with a high-density BP unit in the surface. When the MPC concentration in a feed is also high, the self-initiated surface graft polymerization between the radicals on the PEEK surface and the MPC monomer occurs extremely rapidly in the reaction system, forming the high-density graft chain on the surface. Hence, diffusion of the MPC monomer onto the PEEK surface might be interfered by the high-density graft chain because of its high viscosity. When the monomers attached to the PEEK surface were subjected to UV-irradiation, radicals were freely formed on the PEEK surface in the early stage but not in the late stage of polymerization, probably because the high-density grafted polymer chains formed by then blocked the diffusion of the monomer to the PEEK surface. Therefore, it is supposed that the rate of increase in the PMPC-graft layer density changed due to the high concentration of free radicals and monomers.

The water-wettability of the PMPC-grafted PEEK surface is considerably greater than that of the untreated PEEK surface (Fig. 6), because of the presence of a nanometer-scaled PMPC layer (Fig. 4(A)): MPC is a highly hydrophilic compound, while PMPC is water-soluble. In Figs. 4–7, we observe that the dynamic coefficient

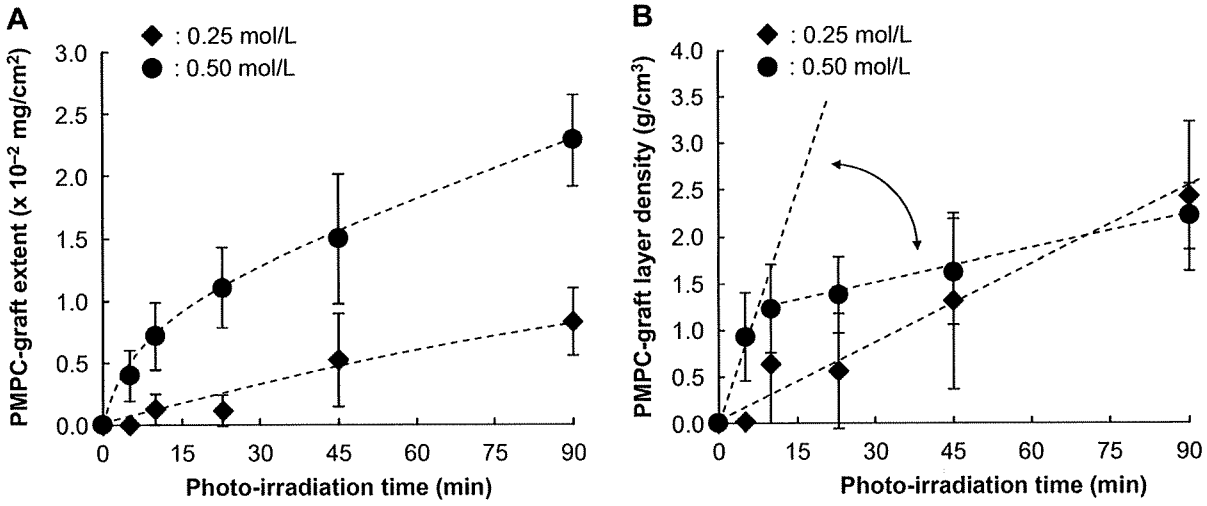


**Fig. 5.** Physical properties ($n = 5$) of PMPC-graft layer on PEEK surface as a function of the photo-irradiation time with MPC concentrations of 0.25 and 0.50 mol/L. (A) PMPC-graft extent by weighting, and (B) density calculated by (A) and mean PMPC-graft layer thickness of Fig. 4(B). Bar: Standard deviation.

of friction was greatly dependent on the water-wettability (static-water contact angle), but virtually independent of the structure (thickness and density) of the graft layer. A significant reduction in the static-water contact angle of the PMPC-grafted surface resulted in a substantial improvement in friction property. Fluid-film lubrication (or hydration lubrication) with the PMPC-grafted surface was achieved by the intermediate hydrated layer. It can be affirmed that this highly lubricated surface utilizing PMPC mimics the natural cartilage structure [33]. When the PEEK surface is modified by PMPC-grafting, the grafted PMPC causes a significant reduction in sliding friction between the graft surfaces because the thin water films that are formed act as extremely efficient lubricants. The water-lubrication systems utilizing PMPC suppress direct contact of the counter-bearing face with the PEEK substrate in order to reduce the frictional force. Thus, the PMPC-graft layer is expected to significantly increase the durability of the bearing biomaterials. On the other hand, when the photo-irradiation time was shorter than 23 min, the decrease in the static-water contact angle of the PMPC-grafted PEEK surface with a 0.25-mol/L MPC concentration was only slight. It was thought that the surface phenomenon was caused by the pinacolization reaction, because the static-water contact angle of the UV-irradiated PEEK surface without monomer was decreased to approximately 80° (data not shown).

The fabrication of surfaces that exhibit anti-protein adsorption and/or cell adhesion has been one of goals of surface engineering for medical devices. The adsorption of the BSA on the PMPC-grafted PEEK surface decreased to 10% ($p < 0.001$) with an increase in photo-irradiation time, as shown in Fig. 8, as compared to that in untreated PEEK. It is shown that the extent of protein rejection is related to the PMPC-graft extent (Figs. 5(A) and 8). Extensive grafting gives rise not only to an increase in the thickness of graft layer but also to an increase in the volume fraction (i.e., density) of graft segments in the layer. Therefore, it was thought that these characteristics of thickness and density of the PMPC-graft layer had a significant influence on protein adsorption. The mechanism of protein adsorption resistance on the PMPC-grafted surface is

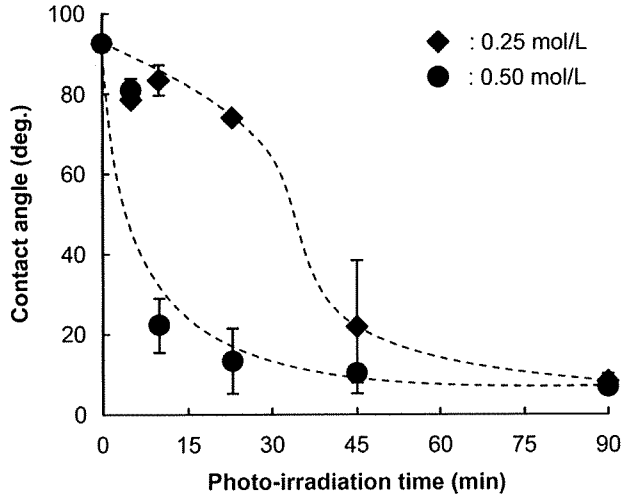


**Fig. 6.** Static-water contact angle ($n = 15$) of PMPC-grafted PEEK as a function of the photo-irradiation time with MPC concentrations of 0.25 and 0.50 mol/L. Bar: Standard deviation.

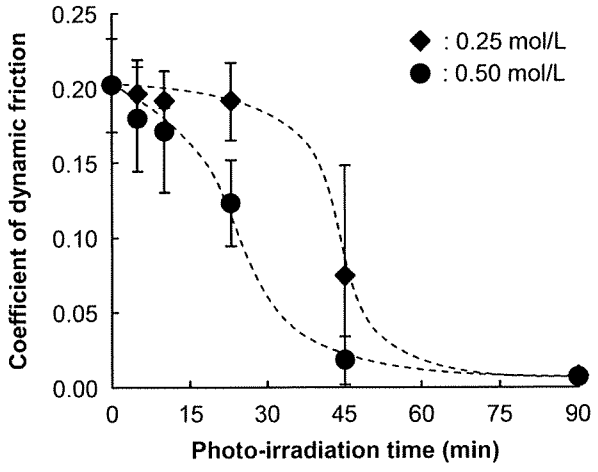


**Fig. 7.** Coefficient of dynamic friction ($n = 5$) of PMPC-grafted PEEK as a function of the photo-irradiation time with MPC concentrations of 0.25 and 0.50 mol/L. Bar: Standard deviation.

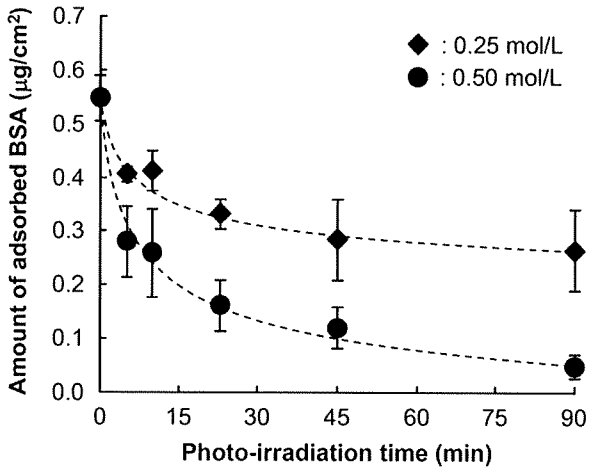


**Fig. 8.** Amount of adsorbed BSA ($n = 3$) of PMPC-grafted PEEK as a function of the photo-irradiation time with MPC concentrations of 0.25 and 0.50 mol/L. Bar: Standard deviation.

hypothesized as follows: the protein adsorption resistance attributed to the water-fluid film and hydration layer was due to water and hydrophilic macromolecules with volume exclusion effects. The presence of the water-fluid film and hydration layer is responsible for the easy detachment of proteins and the prevention of conformational changes in the adsorbed proteins [34]. These observations are consistent with the results of the static-water-contact angle measurements, cross-sectional TEM observations, and PMPC-graft layer weighting of the PEEK whose surface was modified by PMPC-grafting. These results imply that the PMPC-grafted PEEK surface is biocompatible in terms of tissue and blood compatibility, because MPC polymer-modified surfaces are known to exhibit *in vivo* antibiofouling [16,20,23,24].

As shown in Table 1, the mechanical properties of the PEEK are unchanged even after PMPC-grafting. This indicates that the photo-induced radical graft polymerization proceeds only on the surface of the PEEK substrate, while the properties of the substrate remain unchanged. Retention of the properties of the PEEK substrate is very important in clinical use, because the biomaterials used in implants act not only as surface-functional materials but also as structural materials *in vivo*.

The design of a well-characterized surface is a considerably important and difficult task. The photo-induced graft polymerization in the absence of photo-initiators of this study, i.e., "self-initiated surface graft polymerization" successfully prepared the surface with controlled graft layer thickness and density. This simple self-initiated surface graft polymerization would be highly suitable for industrial applications [35,36] as well as the development of medical devices [2–7]. The synthesis of a self-initiated biocompatible polymer having unique properties such as anti-protein adsorption and wettability by the photo-induced grafting-from polymerization reaction is a novel phenomenon in the field of biomaterials and bioengineering sciences, and the fabrication of the PMPC-grafted PEEK surface can result in the development of next-generation multifunctional biomaterials.

**Table 1**
Mechanical properties ($n = 10$) of untreated and PMPC-grafted PEEK.

| Test method | Property | PEEK (untreated) | PMPC-grafted PEEK | *t*-Test |
|---|---|---|---|---|
| Tensile test | Yield strength (MPa) | 109.4 (0.4)[a] | 109.9 (0.6) | N.S. |
| | Ultimate strength (MPa) | 71.5 (1.5) | 71.7 (1.7) | N.S. |
| | Elongation (%) | 24.0 (9.5) | 24.4 (9.0) | N.S. |
| Flexural test | Ultimate strength (MPa) | 168.9 (0.6) | 173.7 (1.8) | <0.05 |
| | Ultimate strain (%) | 6.4 (0.1) | 6.7 (0.2) | <0.05 |
| | Modulus (GPa) | 3.9 (0.0) | 3.9 (0.0) | N.S. |

[a] The standard deviations are shown in parenthesis.

## 5. Conclusions

A biocompatible and highly hydrophilic nanometer-scale-modified surface was successfully fabricated on the PEEK substrate by the photo-induced graft polymerization of PMPC in the absence of photo-initiators, i.e., "self-initiated surface graft polymerization." Since MPC is a highly hydrophilic compound, the water wettability and lubricity of the PMPC-grafted PEEK surface were greater than that of the untreated PEEK surface due to the formation of a PMPC nanometer-scale layer. In addition, the amount of BSA adsorbed on the PMPC-grafted PEEK surface considerably decreased compared to that in the case of untreated PEEK. The density and thickness of the grafting layer could be controlled by the photo-irradiation time and monomer concentration.

## References

[1] Williams DF, McNamara A, Turner RM. Potential of polyetheretherketone (PEEK) and carbon-fibre-reinforced PEEK in medical applications. J Mater Sci Lett 1987;6:188–90.
[2] Kurtz SM, Devine JN. PEEK biomaterials in trauma, orthopedic, and spinal implants. Biomaterials 2007;28(32):4845–69.
[3] Wang A, Lin R, Stark C, Dumbleton JH. Suitability and limitations of carbon fiber reinforced PEEK composites as bearing surfaces for total joint replacements. Wear 1999;225–229:724–7.
[4] Joyce TJ, Rieker C, Unsworth A. Comparative in vitro wear testing of PEEK and UHMWPE capped metacarpophalangeal prostheses. Biomed Mater Eng 2006;16(1):1–10.
[5] Latif AM, Mehats A, Elcocks M, Rushton N, Field RE, Jones E. Pre-clinical studies to validate the MITCH PCR Cup: a flexible and anatomically shaped acetabular component with novel bearing characteristics. J Mater Sci Mater Med 2008;19(4):1729–36.
[6] Yu S, Hariram KP, Kumar R, Cheang P, Aik KK. In vitro apatite formation and its growth kinetics on hydroxyapatite/polyetheretherketone biocomposites. Biomaterials 2005;26(15):2343–52.
[7] Fan JP, Tsui CP, Tang CY, Chow CL. Influence of interphase layer on the overall elasto-plastic behaviors of HA/PEEK biocomposite. Biomaterials 2004;25(23):5363–73.
[8] Kyomoto M, Ishihara K. Self-initiated surface graft polymerization of 2-methacryloyloxyethyl phosphorylcholine on poly(ether-ether-ketone) by photo-irradiation. ACS Appl Mater Interfaces 2009;1(3):537–42.
[9] Giancaterina S, Rossi A, Rivaton A, Gardette JL. Photochemical evolution of poly(ether ether ketone). Polym Degrad Stab 2000;68(1):133–44.
[10] Wang H, Brown HR, Li Z. Aliphatic ketones/water/alcohol as a new photo-initiating system for the photografting of methacrylic acid onto high-density polyethylene. Polymer 2007;48(4):939–48.
[11] Yang W, Rånby B. Photoinitiation performance of some ketones in the LDPE–acrylic acid surface photografting system. Eur Polym J 1999;35(8):1557–68.
[12] Qiu C, Nguyen QT, Ping Z. Surface modification of cardo polyetherketone ultrafiltration membrane by photo-grafted copolymers to obtain nano-filtration membranes. J Membr Sci 2007;295(1–2):88–94.
[13] Nguyen HX, Ishida H. Molecular analysis of the melting behaviour of poly(aryl-ether-ether-ketone). Polymer 1986;27(9):1400–5.
[14] Cole KC, Casella IG. Fourier transform infrared spectroscopic study of thermal degradation in films of poly(etheretherketone). Thermochim Acta 1992;211:209–28.
[15] Qiu KY, Si K. Grafting reaction of macromolecules with pendant amino groups via photoinitiation with benzophenone. Macromol Chem Phys 1996;197:2403–13.
[16] Moro T, Takatori Y, Ishihara K, Konno T, Takigawa Y, Matsushita T, et al. Surface grafting of artificial joints with a biocompatible polymer for preventing periprosthetic osteolysis. Nat Mater 2004;3:829–37.
[17] Moro T, Takatori Y, Ishihara K, Nakamura K, Kawaguchi H. 2006 Frank Stinchfield Award: grafting of biocompatible polymer for longevity of artificial hip joints. Clin Orthop Relat Res 2006;453:58–63.
[18] Moro T, Kawaguchi H, Ishihara K, Kyomoto M, Karita T, Ito H, et al. Wear resistance of artificial hip joints with poly(2-methacryloyloxyethyl phosphorylcholine) grafted polyethylene: comparisons with the effect of polyethylene cross-linking and ceramic femoral heads. Biomaterials 2009;30(16):2995–3001.
[19] Sibarani J, Takai M, Ishihara K. Surface modification on microfluidic devices with 2-methacryloyloxyethyl phosphorylcholine polymers for reducing unfavorable protein adsorption. Colloids Surf B Biointerfaces 2007;54(1):88–93.

[20] Ueda T, Oshida H, Kurita K, Ishihara K, Nakabayashi N. Preparation of 2-methacryloyloxyethyl phosphorylcholine copolymers with alkyl methacrylates and their blood compatibility. Polym J 1992;24(11):1259–69.
[21] Konno T, Ishihara K. Temporal and spatially controllable cell encapsulation using a water-soluble phospholipid polymer with phenylboronic acid moiety. Biomaterials 2007;28(10):1770–7.
[22] Xu Y, Takai M, Konno T, Ishihara K. Microfluidic flow control on charged phospholipid polymer interface. Lab Chip 2007;7(2):199–206.
[23] Snyder TA, Tsukui H, Kihara S, Akimoto T, Litwak KN, Kameneva MV, et al. Preclinical biocompatibility assessment of the EVAHEART ventricular assist device: coating comparison and platelet activation. J Biomed Mater Res A 2007;81(1):85–92.
[24] Ueda H, Watanabe J, Konno T, Takai M, Saito A, Ishihara K. Asymmetrically functional surface properties on biocompatible phospholipid polymer membrane for bioartificial kidney. J Biomed Mater Res A 2006;77(1):19–27.
[25] Kyomoto M, Moro T, Konno T, Takadama H, Yamawaki N, Kawaguchi H, et al. Enhanced wear resistance of modified cross-linked polyethylene by grafting with poly(2-methacryloyloxyethyl phosphorylcholine). J Biomed Mater Res A 2007;82(1):10–7.
[26] Ishihara K, Ueda T, Nakabayashi N. Preparation of phospholipid polymers and their properties as polymer hydrogel membranes. Polym J 1990;22(5):355–60.
[27] He D, Susanto H, Ulbricht M. Photo-irradiation for preparation, modification and stimulation of polymeric membranes. Prog Polym Sci 2009;34:62–98.
[28] ASTM F2026-02: Standard specification for polyetheretherketone (PEEK) polymers for surgical implant applications. In: Arendt SA, Bailey SJ, editors. Annual book of ASTM standards, vol. 13, 2004.
[29] Kyomoto M, Moro T, Iwasaki Y, Miyaji F, Kawaguchi H, Takatori Y, et al. Superlubricious surface mimicking articular cartilage by grafting poly (2-methacryloyloxyethyl phosphorylcholine) on orthopaedic metal bearings. J Biomed Mater Res A 2009;91(3):730–41.
[30] Matsuda T, Kaneko M, Ge S. Quasi-living surface graft polymerization with phosphorylcholine group(s) at the terminal end. Biomaterials 2003;24: 4507–15.
[31] Braunecker WA, Matyjaszewski K. Controlled/living radical polymerization: features, developments, and perspectives. Prog Polym Sci 2007;32(1): 93–146.
[32] Kyomoto M, Moro T, Miyaji F, Hashimoto M, Kawaguchi H, Takatori Y, et al. Effect of 2-methacryloyloxyethyl phosphorylcholine concentration on photo-induced graft polymerization of polyethylene in reducing the wear of orthopaedic bearing surface. J Biomed Mater Res A 2008;86(2):439–47.
[33] Ishikawa Y, Hiratsuka K, Sasada T. Role of water in the lubrication of hydrogel. Wear 2006;261:500–4.
[34] Kyomoto M, Moro T, Miyaji F, Hashimoto M, Kawaguchi H, Takatori Y, et al. Effects of mobility/immobility of surface modification by 2-methacryloyloxyethyl phosphorylcholine polymer on the durability of polyethylene for artificial joints. J Biomed Mater Res A 2009;90(2):362–71.
[35] Hasegawa S, Suzuki Y, Maekawa Y. Preparation of poly(ether ether ketone)-based polymer electrolytes for fuel cell membranes using grafting technique. Radiat Phys Chem 2008;77:617–21.
[36] Chen J, Asano M, Maekawa Y, Yoshida M. Fuel cell performance of polyetheretherketone-based polymer electrolyte membranes prepared by a two-step grafting method. J Membr Sci 2008;319:1–4.

Biomaterials 31 (2010) 658–668

Contents lists available at ScienceDirect

Biomaterials

journal homepage: www.elsevier.com/locate/biomaterials

# Lubricity and stability of poly(2-methacryloyloxyethyl phosphorylcholine) polymer layer on Co–Cr–Mo surface for hemi-arthroplasty to prevent degeneration of articular cartilage

Masayuki Kyomoto [a,c,f], Toru Moro [c,d], Ken-ichi Saiga [a,c,f], Fumiaki Miyaji [f], Hiroshi Kawaguchi [d], Yoshio Takatori [c,d], Kozo Nakamura [d], Kazuhiko Ishihara [a,b,e,*]

[a] Department of Materials Engineering, The University of Tokyo, 7-3-1 Hongo, Bunkyo-ku, Tokyo 113-8654, Japan
[b] Department of Bioengineering, School of Engineering, The University of Tokyo, 7-3-1 Hongo, Bunkyo-ku, Tokyo 113-8654, Japan
[c] Division of Science for Joint Reconstruction, Graduate School of Medicine, The University of Tokyo, 7-3-1 Hongo, Bunkyo-ku, Tokyo 113-8654, Japan
[d] Sensory & Motor System Medicine, Faculty of Medicine, The University of Tokyo, 7-3-1 Hongo, Bunkyo-ku, Tokyo 113-8654, Japan
[e] Center for NanoBio Integration, The University of Tokyo, 7-3-1 Hongo, Bunkyo-ku, Tokyo 113-8654, Japan
[f] Research Department, Japan Medical Materials Corporation, 3-3-31 Miyahara, Yodogawa-ku, Osaka 532-0003, Japan

ARTICLE INFO

*Article history:*
Received 30 July 2009
Accepted 22 September 2009
Available online 9 October 2009

*Keywords:*
Phosphorylcholine
Cobalt alloy
Hip replacement prosthesis
Surface modificaiton
Cartilage
Friction

ABSTRACT

Migration of the artificial femoral head to the inside of the pelvis due to the degeneration of acetabular cartilage has emerged as a serious issue in resurfacing or bipolar hemi-arthroplasty. Surface modification of cobalt–chromium–molybdenum alloy (Co–Cr–Mo) is one of the promising means of improving lubrication for preventing the migration of the artificial femoral head. In this study, we systematically investigated the surface properties, such as lubricity, biocompatibility, and stability of the various modification layers formed on the Co–Cr–Mo with the biocompatible 2-methacryloyloxyethyl phosphorylcholine (MPC) polymer by dip coating or grafting. The cartilage/poly(MPC) (PMPC)-grafted Co–Cr–Mo interface, which mimicked a natural joint, showed an extremely low friction coefficient of <0.01, as low as that of a natural cartilage interface. Moreover, the long-term stability in water was confirmed for the PMPC-grafted layer; no hydrolysis of the siloxane bond was observed throughout soaking in phosphate-buffered saline for 12 weeks. The PMPC-grafted Co–Cr–Mo femoral head for hemi-arthroplasty is a promising option for preserving acetabular cartilage and extending the duration before total hip arthroplasty.



## 1. Introduction

Resurfacing or bipolar hemi-arthroplasty for the treatments of osteoarthritis or osteonecrosis of hip of the young, active patient profile, and fractures of the femur neck of the typically aged patient profile, has long been advocated [1]. Consequently, resurfacing and bipolar hemi-arthroplasties can be possibly used as delaying tactics prior to revision surgeries of total hip arthroplasty. Most patients receive dramatic pain relief and rapid improvement in both their daily activities and quality of life due to advantages such as reduced blood loss, lower dislocation, ease of implantation, etc. However, migration of the artificial femoral head to the inside of the pelvis due to the degeneration of acetabular cartilage has emerged as a serious issue in the hemi-arthroplasties [2]. The longevity of the artificial femoral head after hemi-arthroplasty depends upon the quality of the acetabular cartilage or the lubrication conditions between the artificial femoral head and acetabular cartilage. Surface modifications of cobalt–chromium–molybdenum alloy (Co–Cr–Mo) for the artificial femoral head is one of the promising means of improving lubrication and preventing the degradation of acetabular cartilage, thereby preventing the migration of the artificial femoral head. Such surface modifications may improve hemi-arthroplasty survival, and liberate the restrictions for its application to younger, active patients.

Most frequently, surface modification with polymer is performed using either of the following methods: (1) surface-initiated graft polymerization, termed as the "grafting from" method, in which monomers are polymerized from initiators, and the polymeric molecules are grafted onto the substrate through covalent bonding; and (2) adsorption or immobilization of the polymer onto

* Corresponding author. Department of Materials Engineering, School of Engineering, The University of Tokyo, Hongo 7-3-1, Bunkyo-ku, Tokyo 113-8656, Japan. Tel.: +81 3 5841 7124; fax: +81 3 5841 8647.
*E-mail address:* ishihara@mpc.t.u-tokyo.ac.jp (K. Ishihara).

0142-9612/$ – see front matter © 2009 Elsevier Ltd. All rights reserved.
doi:10.1016/j.biomaterials.2009.09.083

the substrate (i.e., dipping, cross-linking, and ready-made polymers with reactive end groups reacting with the functional groups of the substrate) [3–5].

2-Methacryloyloxyethyl phosphorylcholine (MPC) polymers have attracted considerable attention as surface modifiable polymers for several medical devices [6–16]. MPC is a monomer for preparing novel polymer biomaterials and can undergo conventional radical copolymerization with other methacrylates, such as *n*-butyl methacrylate (BMA), *n*-dodecyl methacrylate (DMA), and 3-methacryloxypropyl trimethoxysilane (MPSi), to form poly (MPC-*co*-BMA), poly(MPC-*co*-DMA), and poly(MPC-*co*-MPSi), respectively [10–16]. They have potential applications in a variety of fields such as biomedical science, surface science, and bioengineering because they possess unique properties such as excellent anti-biofouling ability and low friction ability. Thus, surface modification with the MPC polymer on medical devices is effective for obtaining biocompatibility. In fact, several medical devices have already been developed by utilizing MPC polymers and used clinically; therefore, the efficacy and safety of MPC polymers as biomaterials are well established [14–16].

In this study, we hypothesize that the structure of surface modification layers might affect the long-term stability, hydration kinetics, articular cartilage retention, etc., and particularly that the poly(MPC) (PMPC)-grafted surface might assure the long-term performance of the artificial femoral head for partial hemiarthroplasty. Therefore, we investigated the surface properties of various surface modification layers with the MPC polymer and the effects of the surface properties on the friction of the artificial femoral head against articular cartilage. The results reveal that the structure of the PMPC-grafted layer on the Co–Cr–Mo surface plays an important role in the articular cartilage retention in the long term.

## 2. Materials and methods

### 2.1. Chemicals

MPC was industrially synthesized by using the method reported by Ishihara et al. and supplied by NOF Corp. (Tokyo, Japan) [17]. MPSi was purchased from Shin-Etsu Chemical Co., Ltd. (Tokyo, Japan). Succinic acid and ethanol were purchased from Kanto Chemical Co., Inc. (Tokyo, Japan). 2-Hydroxy-l-[4-(hydroxyethoxy) phenyl]-2-methyl-propan-1-one (DAROCUR 2959; D2959), as a highly efficient radical photoinitiator for ultraviolet (UV) curing, was purchased from Ciba Specialty Chemicals Holding Inc. (Basel, Switzerland) Poly(MPC-*co*-BMA) (PMB30; MPC unit mole fraction = 0.3) [17], poly(MPC-*co*-MPSi) (PMSi90; MPC unit mole fraction = 0.9) [13], and PMPC (for lubricant additive in friction test) were synthesized in ethanol using 2,2′-azobisisobutyronitrile as an initiator by a conventional radical copolymerization method.

### 2.2. Co–Cr–Mo alloy substrate and pretreatments

The Co–Cr–Mo alloy was supplied by Yoneda Advanced Casting Co., Ltd (Takaoka, Japan). This alloy was manufactured according to the ASTM F75 standard specification for the Co–28Cr–6Mo alloy. The Co–Cr–Mo samples were machined and polished so that the average surface roughness was approximately 0.01 μm; this surface was comparable to those of femoral ball products.

The polished Co–Cr–Mo samples were washed with acetone, and then immersed in 35 vol% nitric acid at room temperature for 35 min. This treatment aimed at passivation by surface oxidation; this would lead to the dissolution of certain foreign substance residues and the concentration of the Cr constituent by "resurfacing" [18]. After the nitric acid treatment, the Co–Cr–Mo samples were irradiated with $O_2$ plasma at a 500-W high-frequency output and 150-mL/min $O_2$ gas flow for 5 min by using an $O_2$ plasma etcher (PR500; Yamato Scientific Co., Ltd., Tokyo, Japan). The $O_2$ plasma treatment increased the thickness of the surface oxide layer [18].

### 2.3. MPC polymer coating

The preparation of the MPC polymer-coated Co–Cr–Mo is schematically illustrated in Fig. 1. The physical adsorption of PMB30 was carried out by the solvent evaporation method, where the pretreated Co–Cr–Mo specimens were dipped into ethanol solution containing 0.2 mass% PMB30 ($Mw = 6.0 \times 10^5$) for 10 s for coating and then placed in an ethanol vapor atmosphere at room temperature for 1 h. The coated Co–Cr–Mo specimens were again dipped for 10 s and placed in the ethanol vapor atmosphere at room temperature for 1 h (PMB30-adsorbed Co–Cr–Mo).

The chemical immobilization of PMSi90 was also carried out by the solvent evaporation method. The pretreated Co–Cr–Mo specimens were dipped into ethanol solution containing 0.5 mass% PMSi90 ($Mw = 9.8 \times 10^4$) and 0.063 mg/mL succinic acid for 12 h for the silanization of trimethoxysilane group of PMSi90 and placed in the ethanol vapor atmosphere at room temperature for 1 h. The coated Co–Cr–Mo specimens were annealed in air at 70 °C for 3 h for dehydration (PMSi90-immobilized Co–Cr–Mo).

### 2.4. MPSi silanization and MPC graft polymerization

The preparation of the PMPC-grafted Co–Cr–Mo is schematically shown in Fig. 1. The pretreated Co–Cr–Mo samples were immersed in an ethanol solution containing 5 mass% MPSi, 1 mass% succinic acid, and 0.1 mass% D2959 at room temperature for 12 h for silanization of the trimethoxysilane group. In this study, D2959 was used as a photoinitiator for surface-initiated polymerization so as to be included in the MPSi layer. They were then annealed at 70 °C for 3 h in air for dehydration. MPC was dissolved in degassed pure water to obtain a concentration of 0.5 mol/L. Subsequently, the MPSi (containing D2959)-coated Co–Cr–Mo samples were immersed in MPC aqueous solutions. Photoinduced graft polymerization on the Co–Cr–Mo surface was performed using ultraviolet irradiation (UVL-400HA ultra-high pressure mercury lamp; Riko-Kagaku Sangyo Co., Ltd., Funabashi, Japan) with an intensity of 5 mW/cm$^2$ at 60 °C for 90 min; a filter (Model D-35; Toshiba Co., Tokyo, Japan) was used to restrict the passage of ultraviolet light to wavelengths of 350 ± 50 nm (PMPC-grafted Co–Cr–Mo) [19]. After the polymerization, the PMPC-grafted Co–Cr–Mo samples were removed from the solution, washed with pure water and ethanol, and dried at room temperature. The molecular weight of the PMPC graft chain on the PMPC-grafted Co–Cr–Mo samples could not be determined due to the difficulty in separating the PMPC graft chain from the Co–Cr–Mo substrate. Additional efforts are needed in this aspect.

### 2.5. Articular cartilage from porcine ankle joint

Articular cartilage specimens were harvested from the flat part of the ankle joint of the fresh frozen porcine tibia (age 6–9 months) by using a surgical saw for the friction test. The pin-type (cylinder-shaped with a height of 5 mm and diameter of 9 mm) articular cartilage specimens had approximately a 1-mm cartilage layer and the subcondral bone used for mounting. Throughout the procedure, the articular cartilage surface was hydrated regularly with Dulbecco's phosphate-buffered saline (PBS, pH 7.4, ion strength = 0.15 M; Immuno-Biological Laboratories Co., Ltd., Takasaki, Japan).

### 2.6. Surface analysis of surface-modified Co–Cr–Mo with various MPC polymers

The functional group vibrations of the surface-modified Co–Cr–Mo samples were examined by Fourier-transform infrared (FT-IR) spectroscopy with attenuated total reflection (ATR) equipment. The FT-IR/ATR spectra were obtained using an FT-IR analyzer (FT/IR615; JASCO Co. Ltd., Tokyo, Japan) for 32 scans over the range from 800 to 2000 cm$^{-1}$ at a resolution of 4.0 cm$^{-1}$.

The surface elemental conditions of the surface-modified Co–Cr–Mo samples were analyzed by X-ray photoelectron spectroscopy (XPS). The XPS spectra were obtained using an XPS spectrophotometer (AXIS-HSi165, Kratos/Shimadzu Co., Kyoto, Japan) equipped with a 15-kV Mg-Kα radiation source at the anode. The take-off angle of the photoelectrons was maintained at 90°. Five scans were taken for each sample.

The static-water contact angles on the surface-modified Co–Cr–Mo samples were measured by the sessile drop method using an optical bench-type contact angle goniometer (Model DM300, Kyowa Interface Science Co., Ltd., Saitama, Japan). Drops of purified water (1 μL) were deposited on the surface-modified Co–Cr–Mo surfaces, and the contact angles were directly measured with a microscope after 60 s of dropping. Measurements were repeated fifteen times for each sample, and the average values were regarded as the contact angles.

The surface-modified Co–Cr–Mo samples were stained with rhodamine 6G (Wako Pure Chemical Industries, Ltd., Osaka, Japan) and observed by fluorescence microscopy (FM). According to previous literature, rhodamine 6G effectively stains the MPC polymer, which possesses great structural similarity to lipids [20]. This simple staining technique enables the evaluation of the surface-modified layer with MPC polymer by FM. An aqueous solution of 200 mass ppm rhodamine 6G was used for all the staining experiments. The samples were immersed in the rhodamine 6G solution for 30 s and then removed. Then, they were washed two times consecutively in distilled water for 30 s and then dried. A fluorescence microscope (Axioskop 2 Plus, Carl Zeiss AG, Oberkochen, Germany) was used for FM imaging and examination of all samples. Pseudo-color images were obtained using a charge coupled device (CCD) camera (VB-7010, Keyence Co., Osaka, Japan) and imaging software (VH analyzer 2.51). Lenses with ×10 magnification and appropriate exposure time (approximately 0.1 s) were employed to obtain the best image quality of the various samples.